What are the Kuiper Belt objects telling us about planet formation?

Wladimir Lyra

New Mexico State University

Planet Formation in the Southwest (PFITS+) Collaboration

Center for Star and Planet Formation – Copenhagen
Sept 23rd, 2025

Structure of the Kuiper Belt

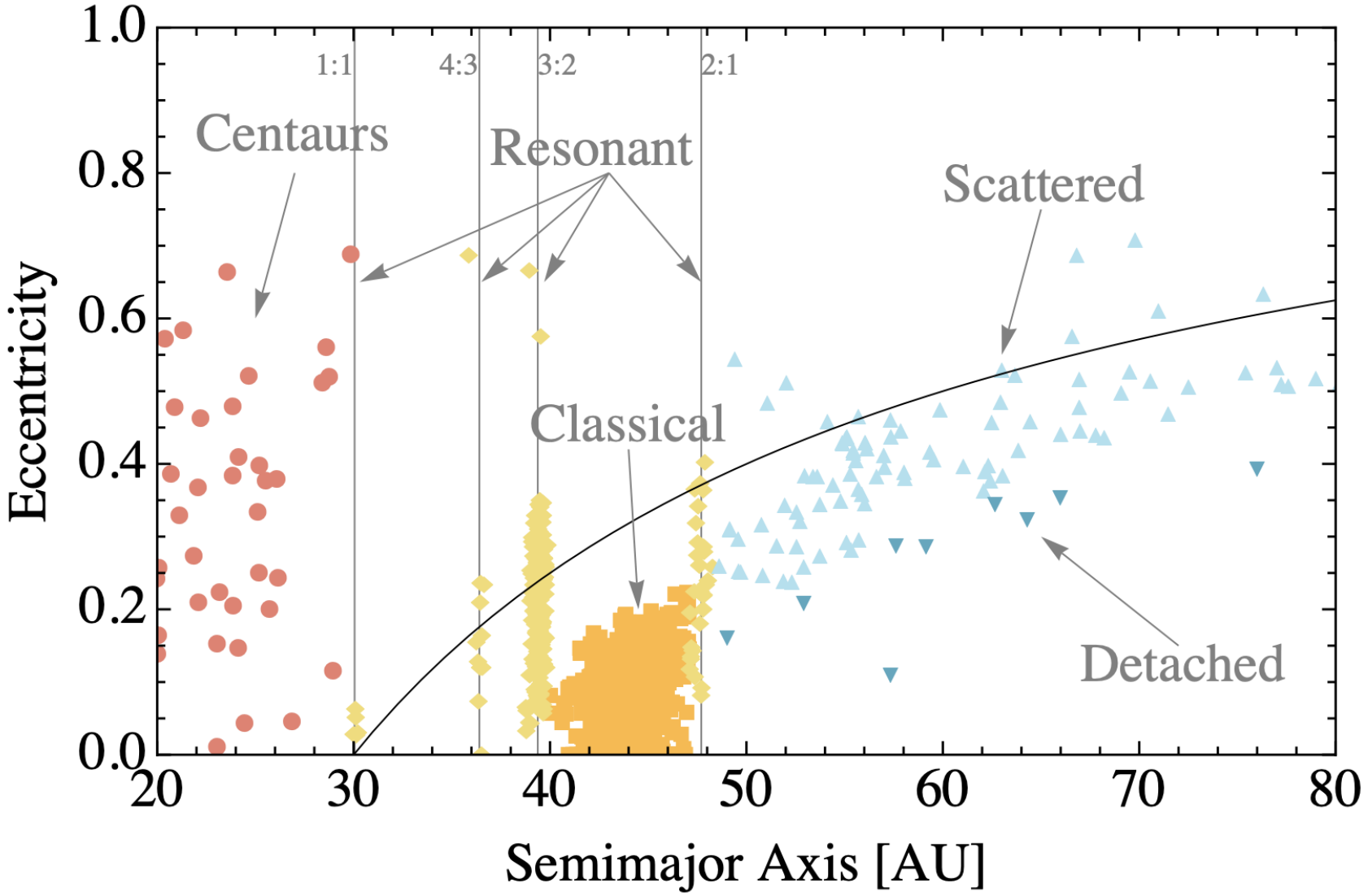

Gladman+ ‘08, Lacerda ‘09, Batygin+ ’10, Dawson & Murray-Clay ‘12

Structure of the Kuiper Belt

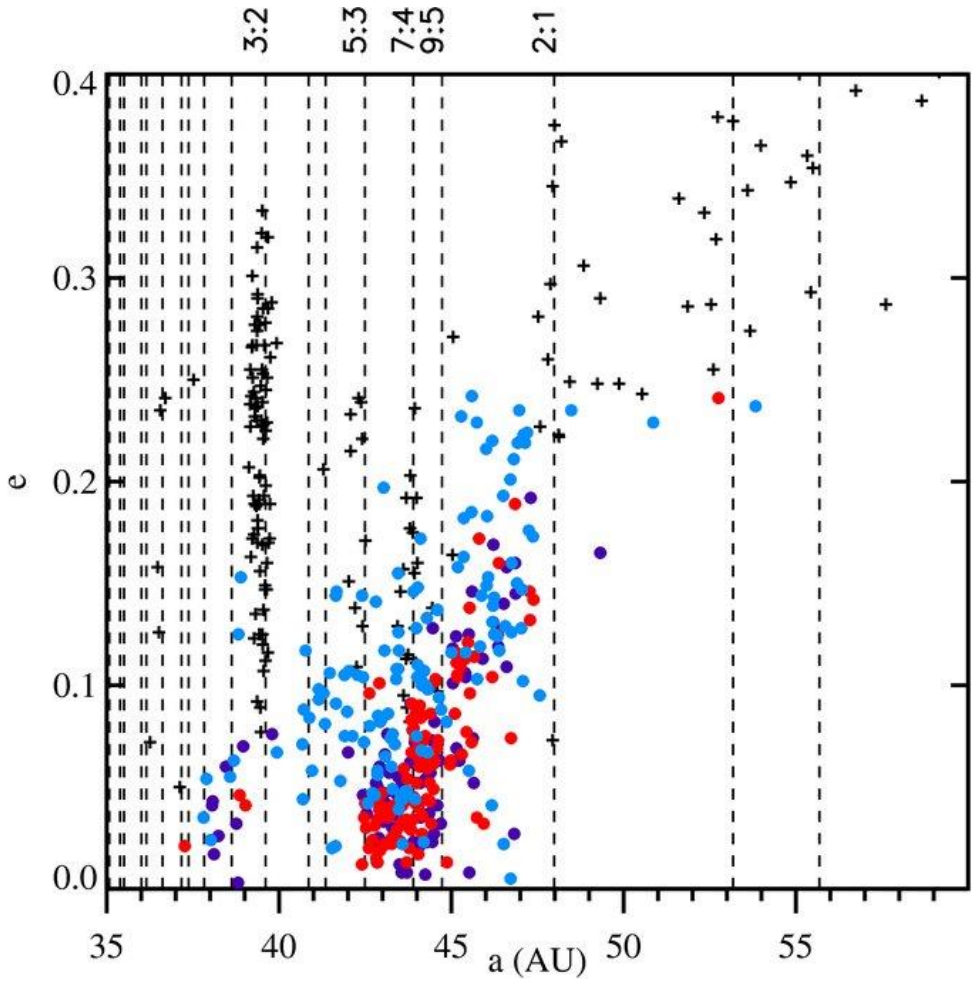

+ Resonant and Scattered
Cold Classical $i<2^o$
"Ambiguous" $2^o<i<6^o$
Hot Classicals $i>6^o$

Cold Classicals: Presumably pristine planetesimals

Gladman+ '08, Lacerda '09, Batygin+ '10, Dawson & Murray-Clay '12

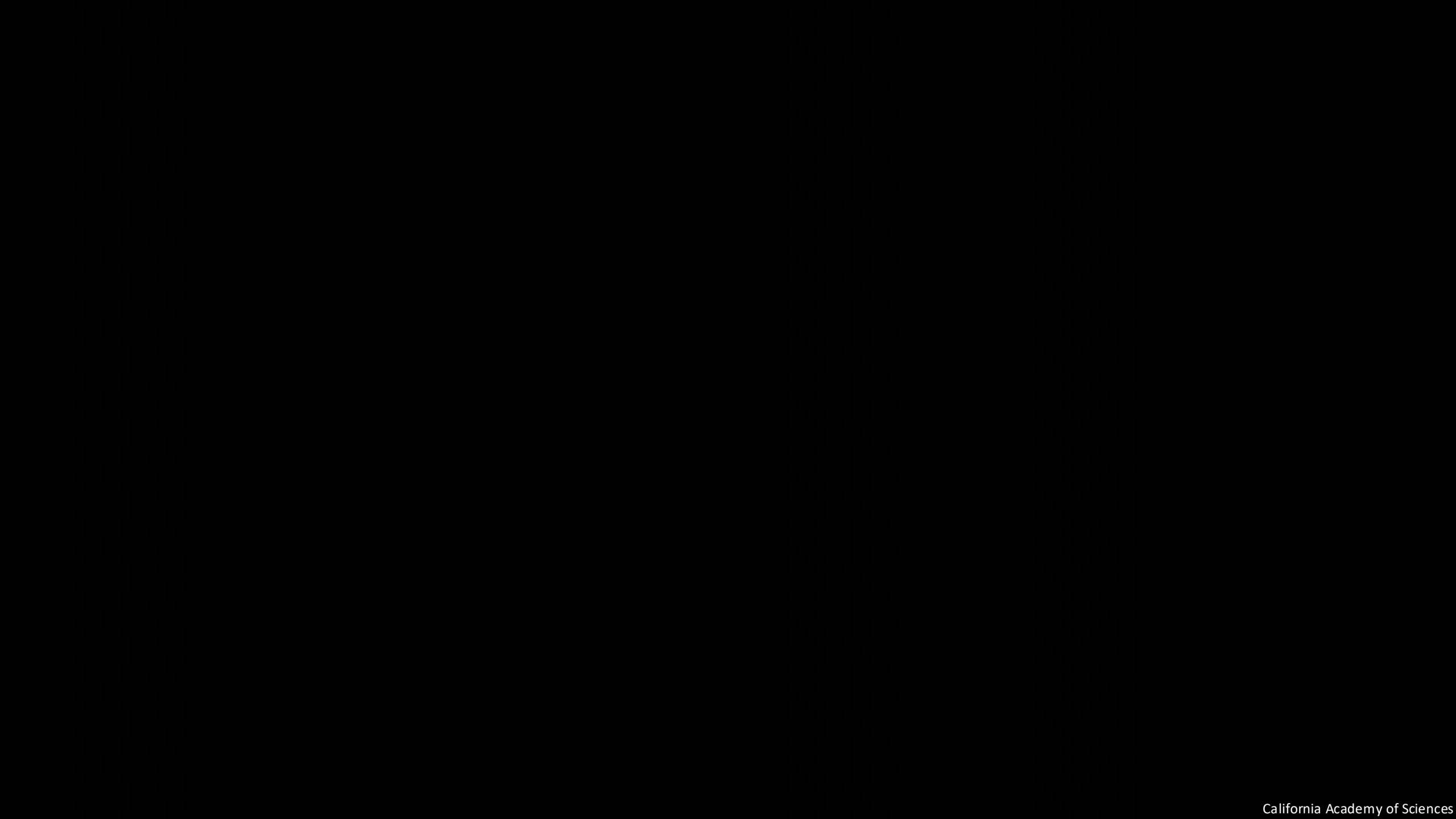

California Academy of Sciences

Arrokoth (MU_{69})

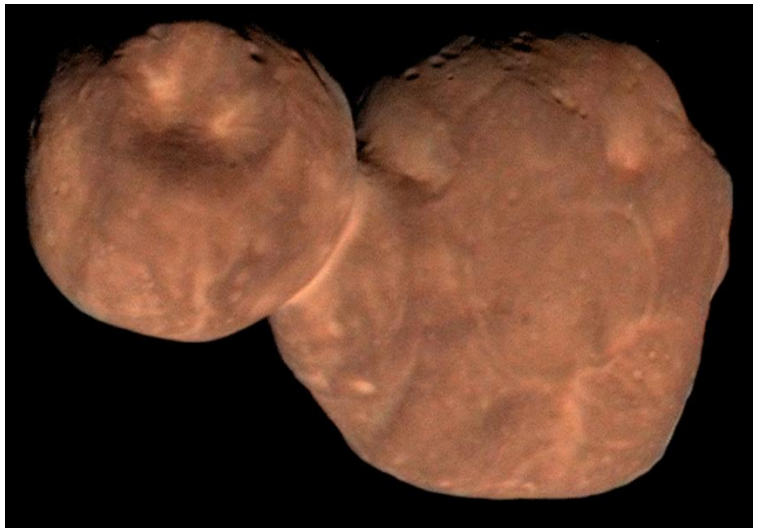

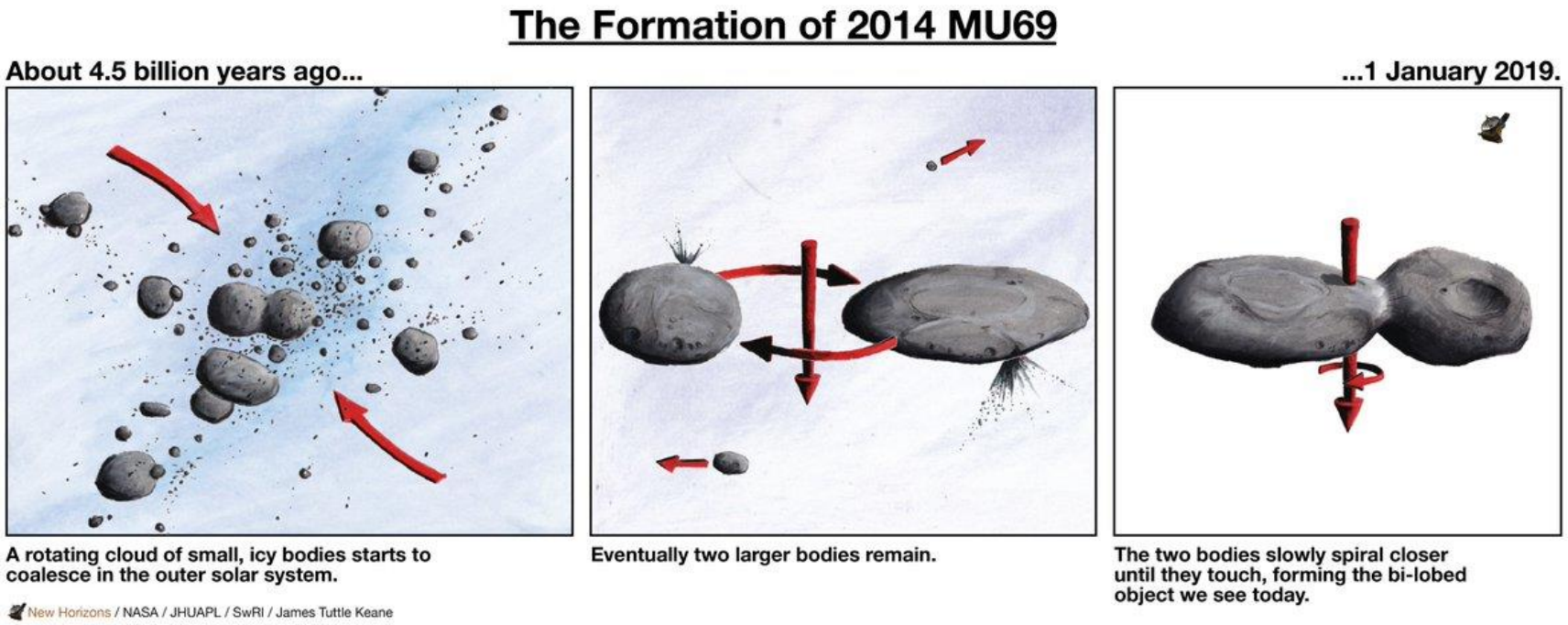

New Horizons Flyby, Jan 2019

Sketch by J.T. Keane

Arrokoth and Pluto ices are different

Arrokoth : Methanol, H_20, HCN

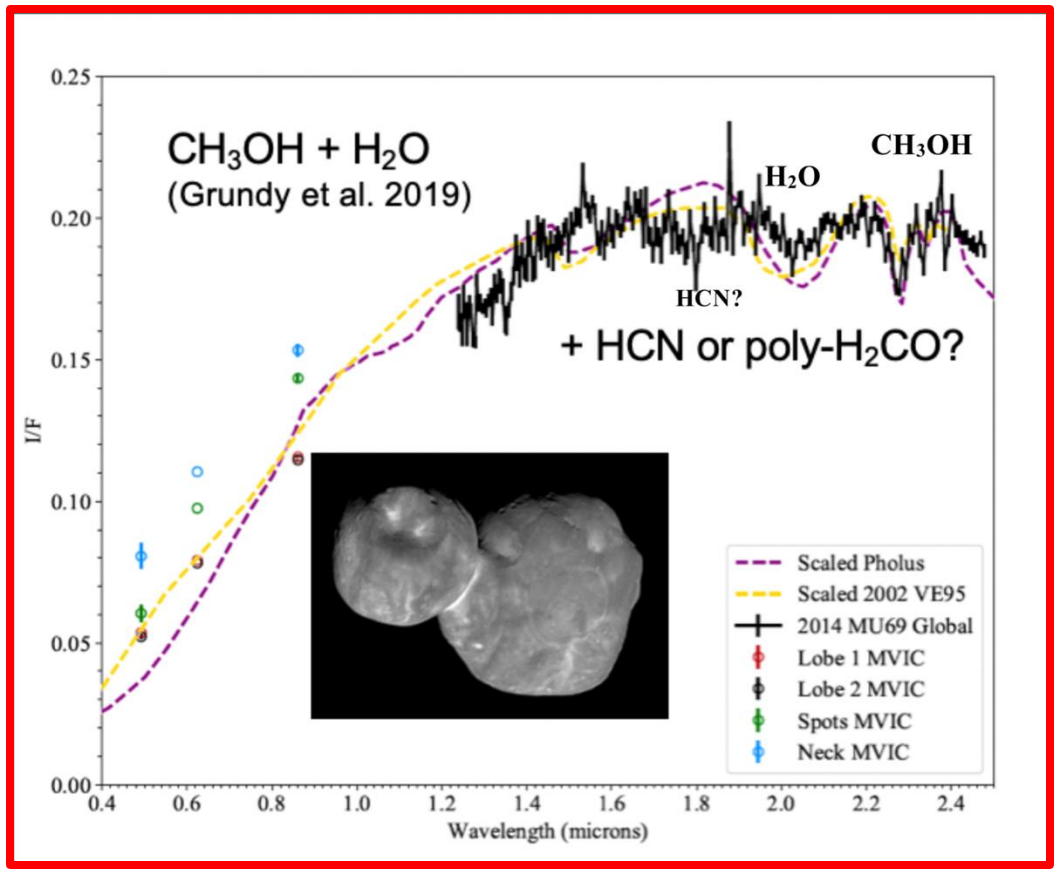

Pluto : CH_4, N_2, CO

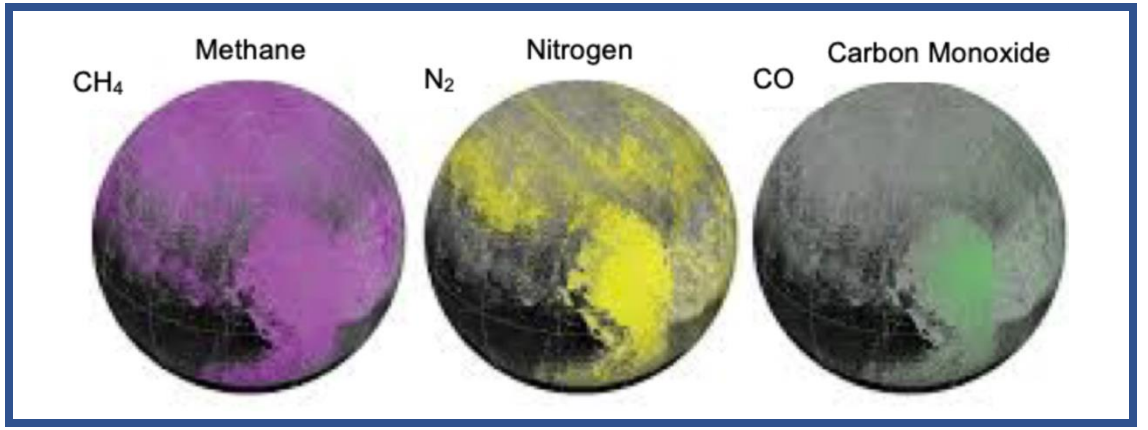

Grundy+ '16, Lisse+ '20

Retention of volatiles

Arrokoth formed with volatiles but lost them

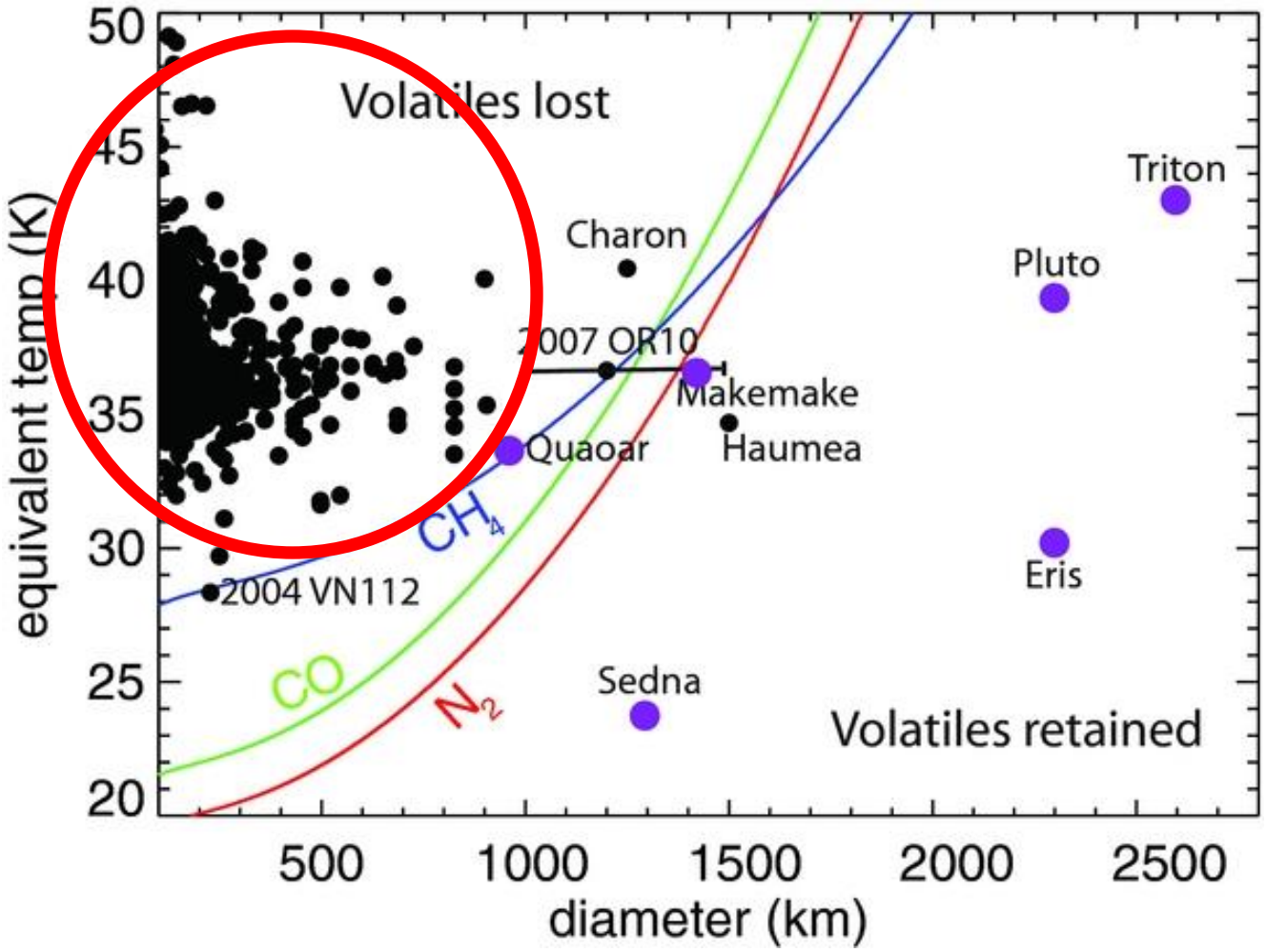

Brown et al. (2011); Lisse et al. (2020)

Retention of volatiles

Pluto cannot have been formed by accumulation of bodies like Arrokoth

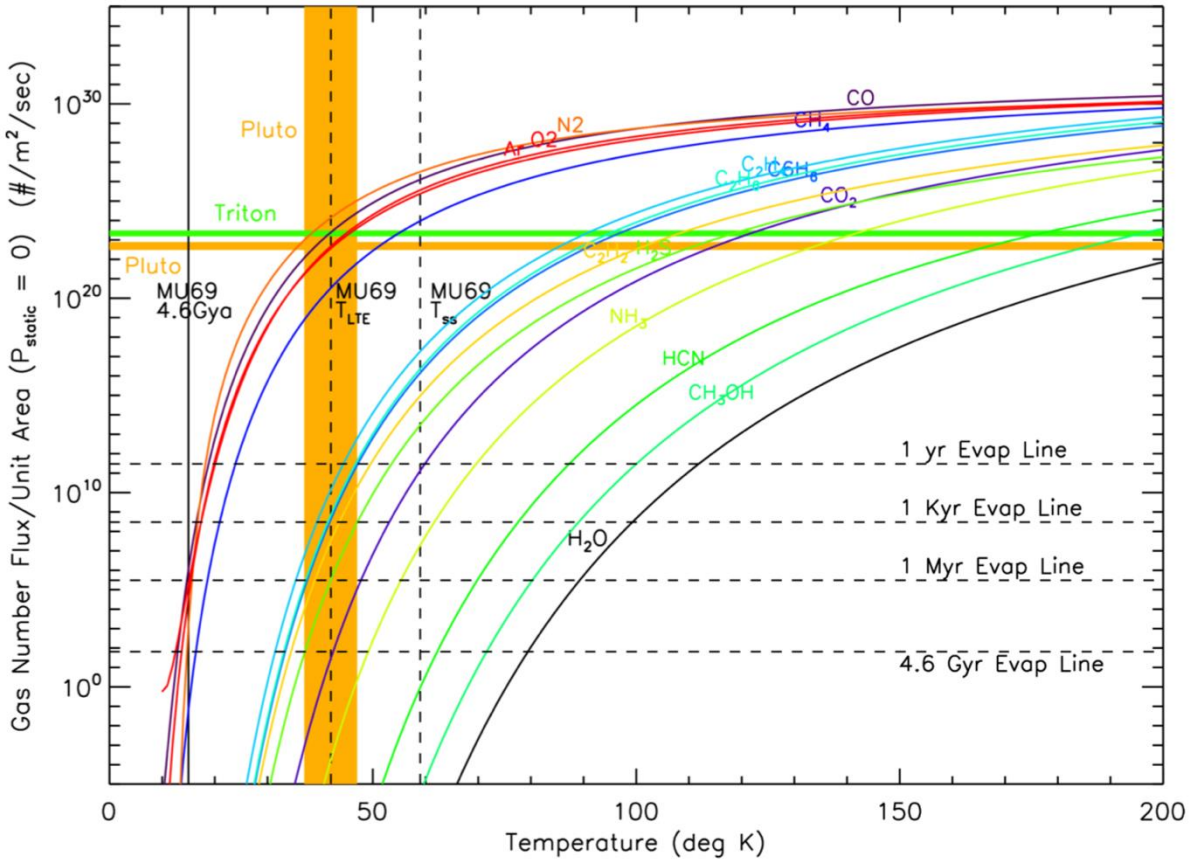

Hypervolatiles (CH_4 / CO / N_2)

Lost under vacuum pressure and microgravity in ~1 Myr for 40 K

Retained for long times only for T < 20K

Arrokoth hypervolatiles lost when disk dissipates and temperature rises to 40K.

Hypervolatile-rich **Pluto cannot form via planetesimal accretion**

Lisse et al. (2020)

The size-density relationship of Kuiper Belt objects

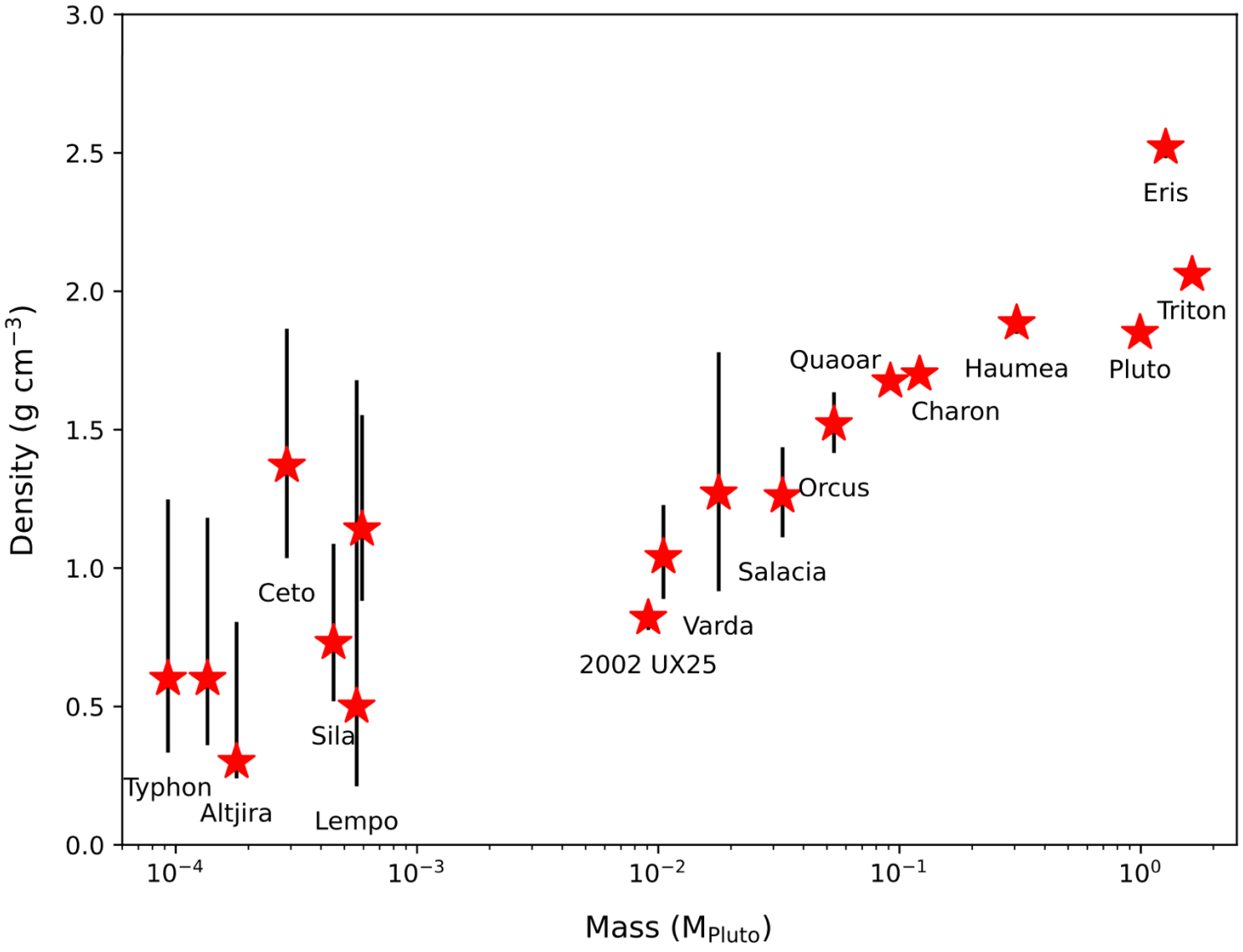

Brown (2013), McKinnon et al. (2017), Noll et al. (2020), Cañas & Lyra + (2024)

Data; *Thomas (2000), Stansberry et al. (2006), Grundy et al. (2007), Brown et al. (2011), Stansberry et al. (2012), Brown (2013), Fornasier et al. (2013), Vilenius, et al. (2014), Nimmo et al. (2016), Ortiz et al. (2017), Brown and Butler (2017), Grundy et al. (2019), Morgado et al. (2023), Pereira et al. (2023).*

Previous best bet:
Porosity removal by gravitational compaction

Problem

- Timing! ^{26}Al would melt if formed within 4 Myr

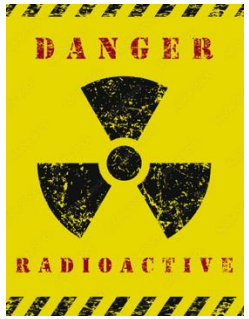

Assumptions

- ~~Constant composition at birth and growth~~
- ~~Growth by planetesimal accretion~~

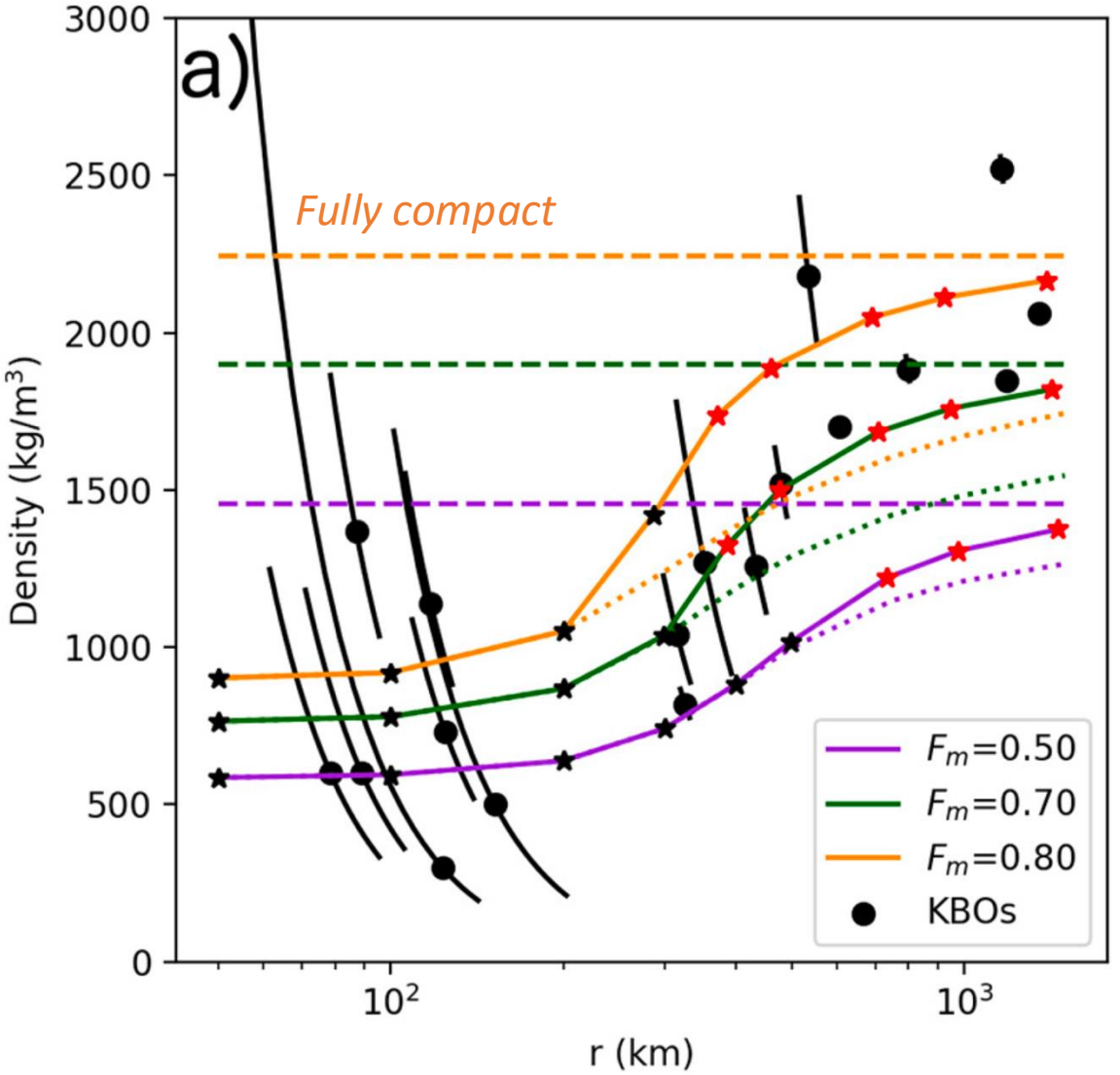

F_m = rock mass fraction

Bierson & Nimmo (2019)

Thermal and photo-desorption

Heating and UV irradiation remove ice
on Myr timescales (Harrison & Schoen 1967).

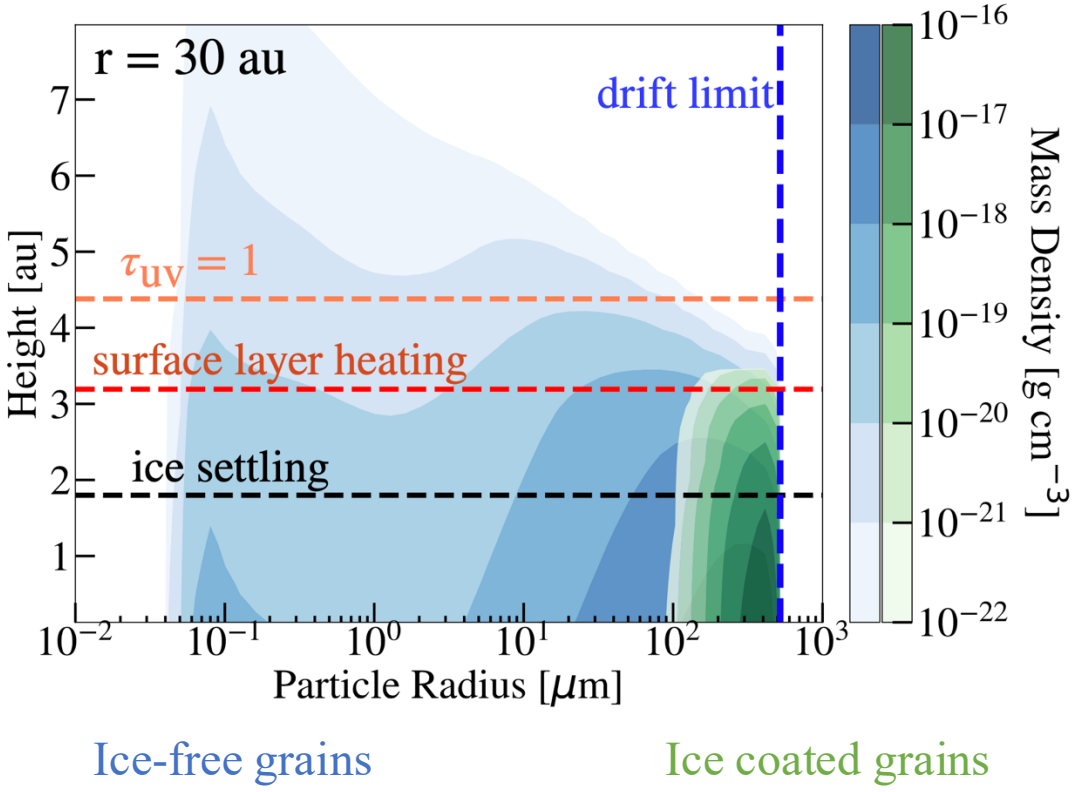

Ice-free grains

Ice coated grains

Powell et al. (2022)

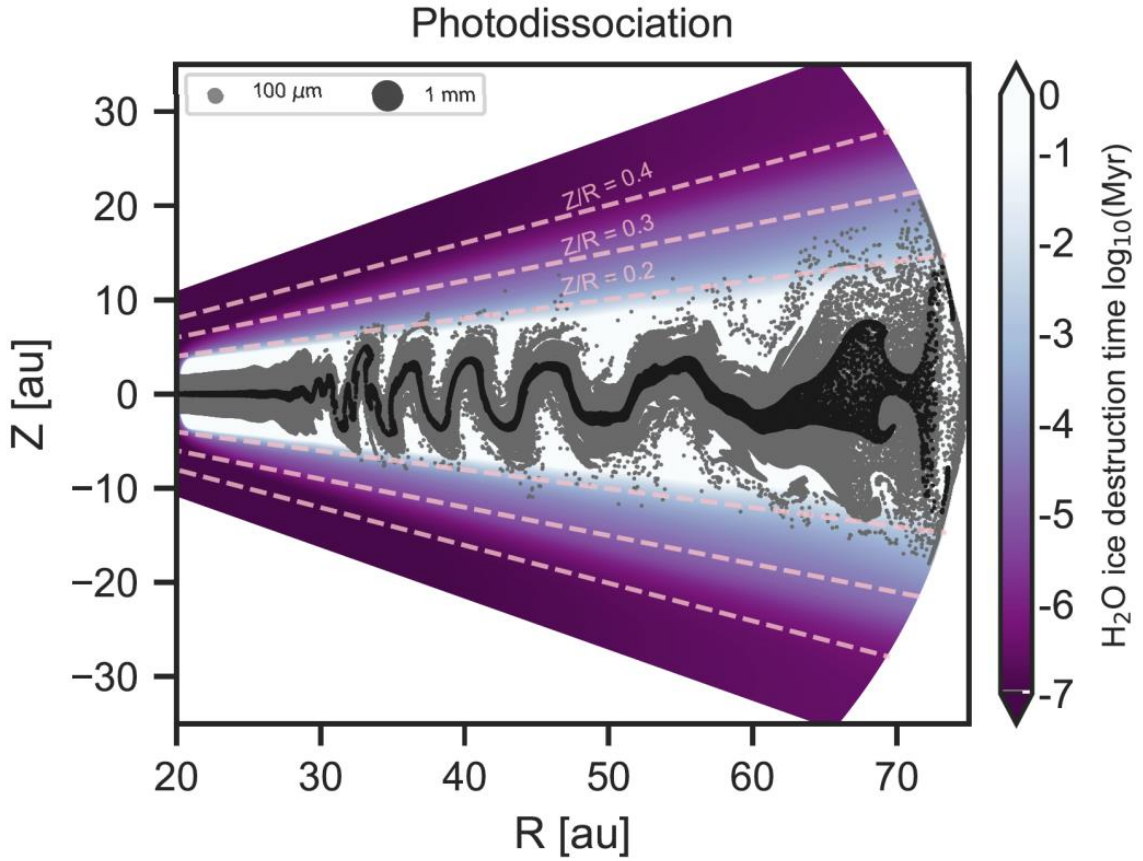

Flores-Rivera et al. (2025)

Thermal and photo-desorption

Evidence in disks

Debris disks

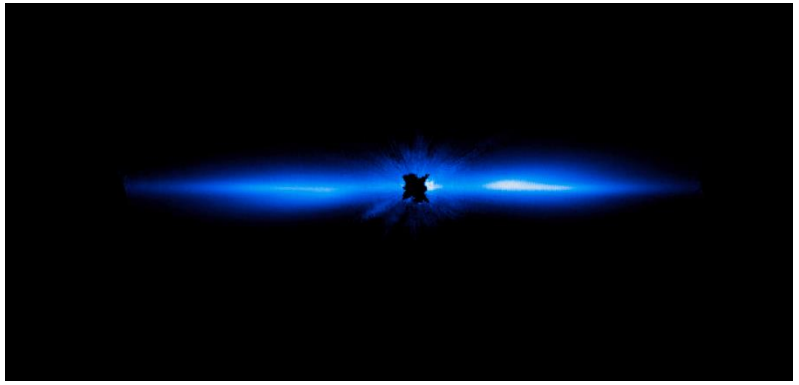

Only upper limits for ice in β Pic
(Ballering et al. 2016, Cavallius et al 2019)

Primordial disks

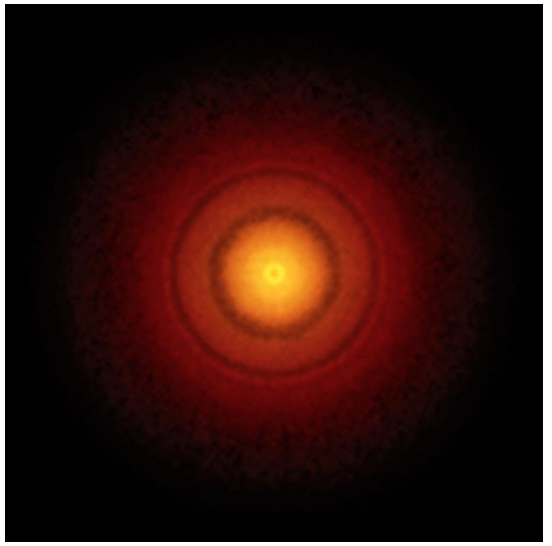

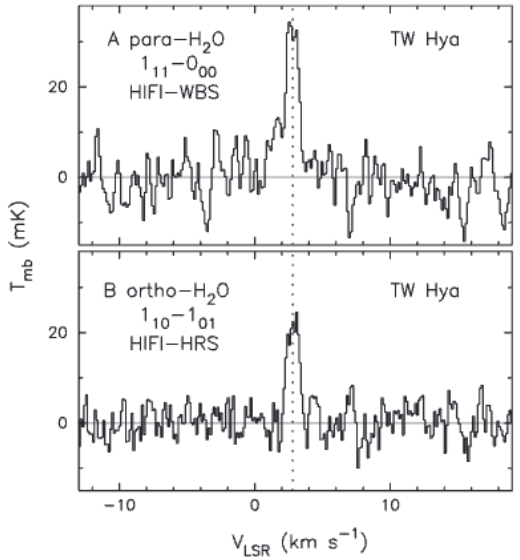

Water vapor observed at large distances for TW Hya
(Hogerheijde et al. 2011, 2012)

Toy model

Small grains lofted in the atmosphere lose ice
Big grains are shielded and remain icy.

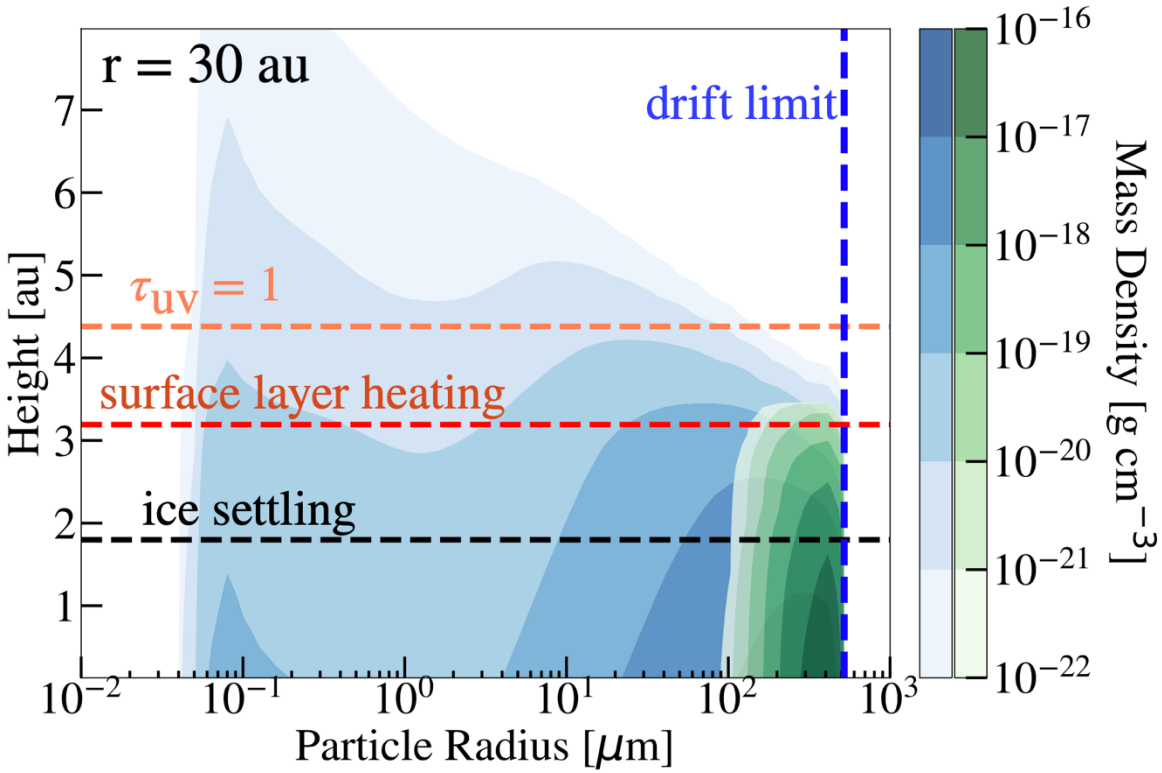

Powell et al. (2022)

Split into icy and silicate pebbles

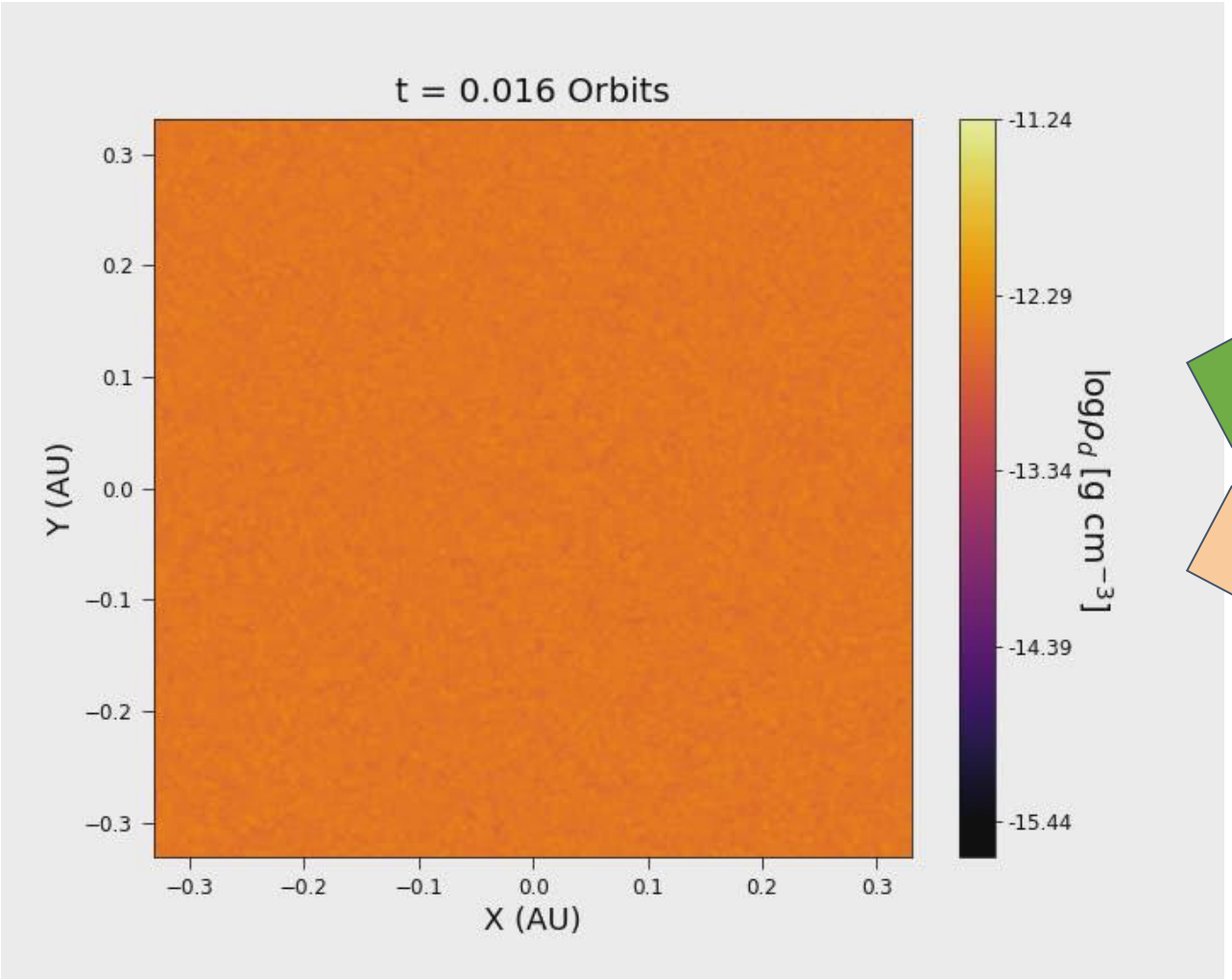

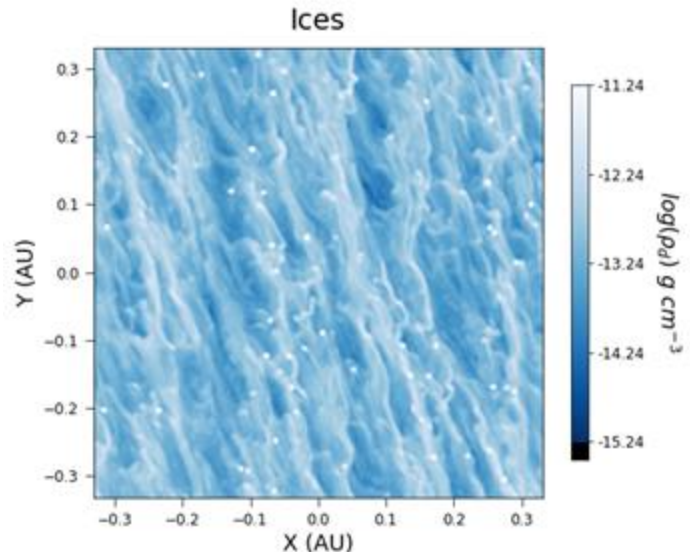

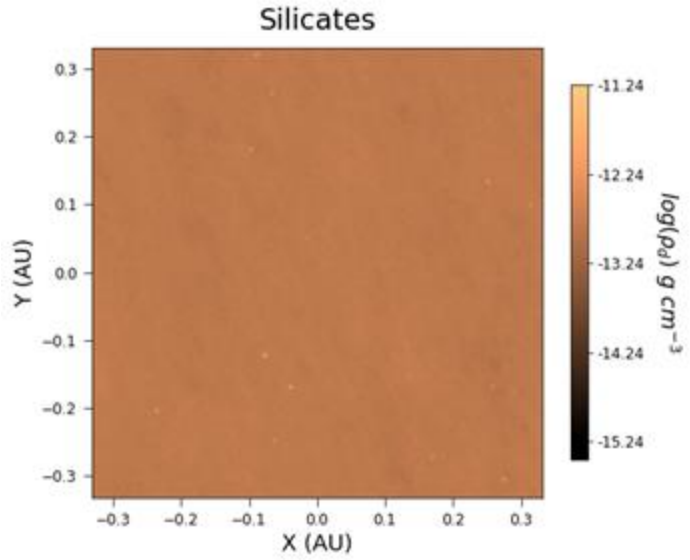

Canas & Lyra + (2024)

The first planetesimals are icy

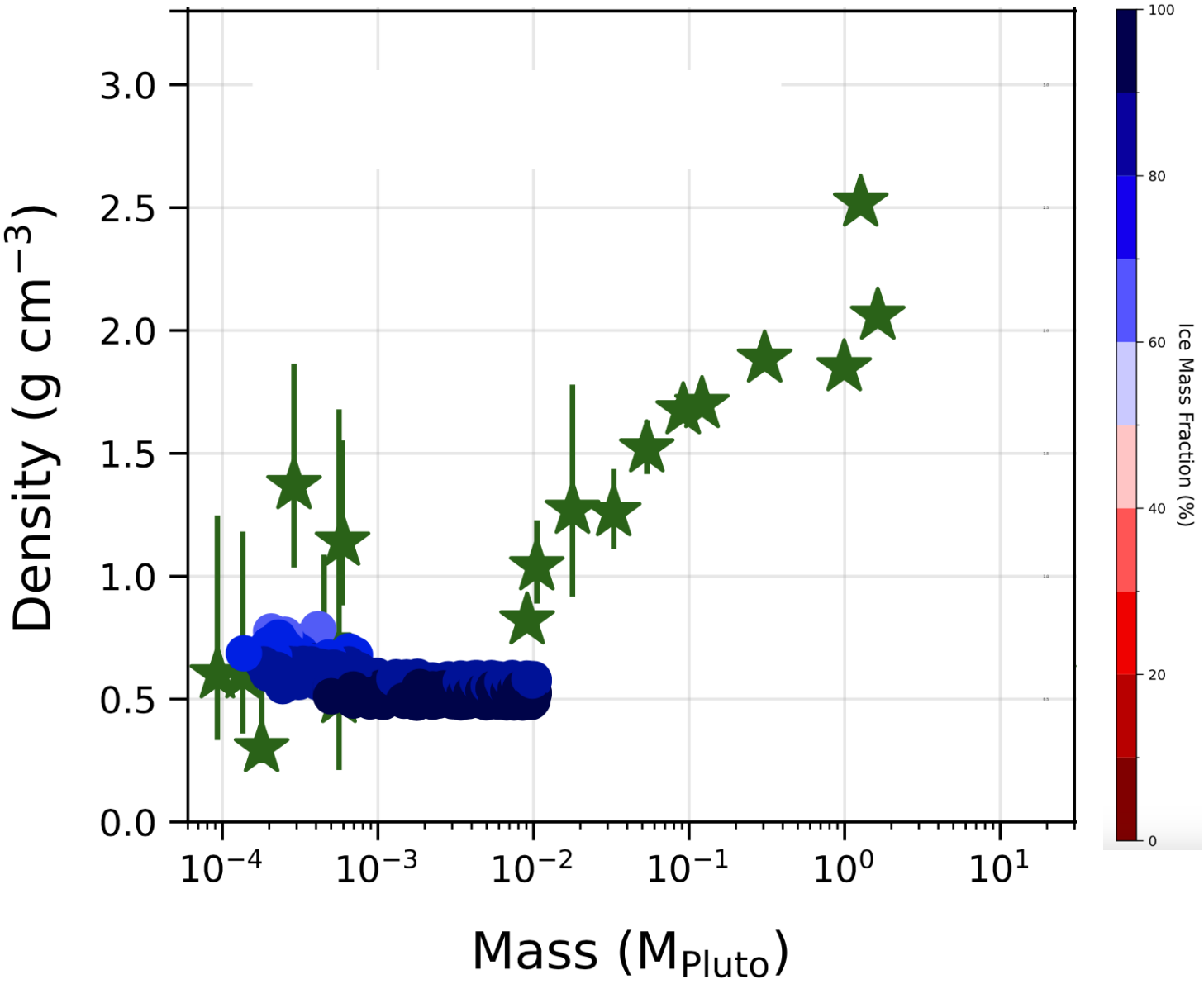

Canas & Lyra + (2024)

^{26}Al binds to silicates: the first planetesimals won't melt

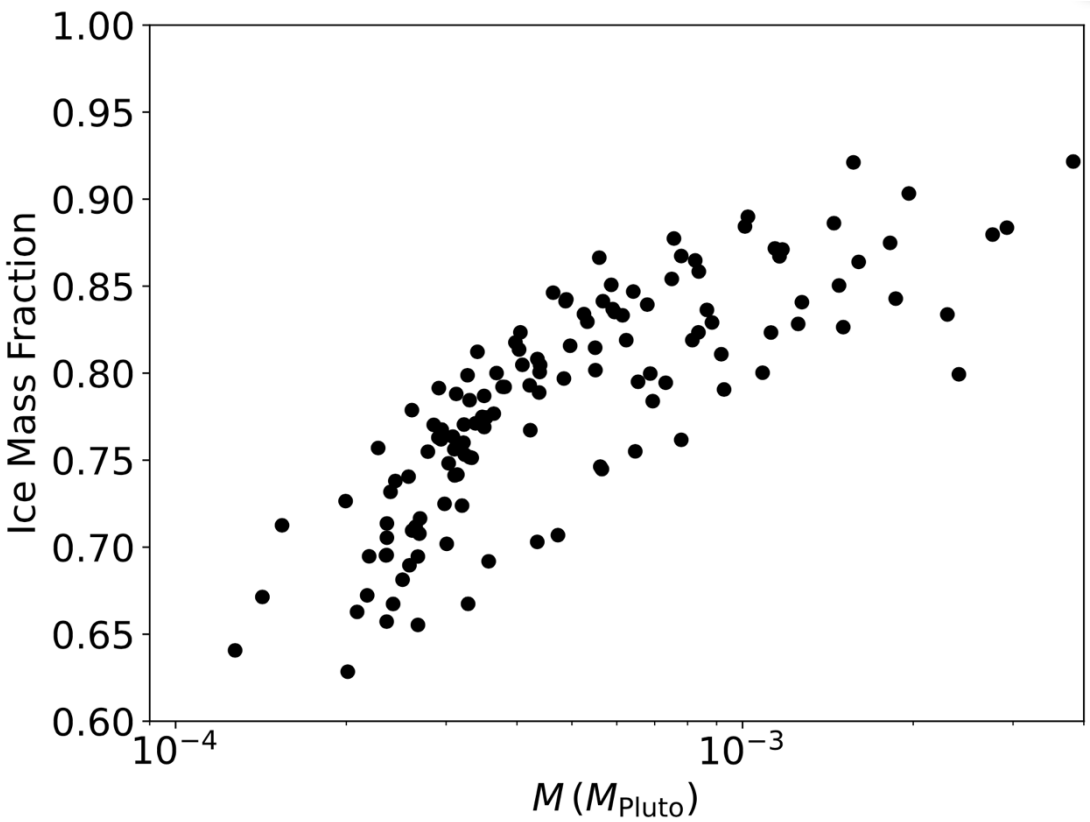

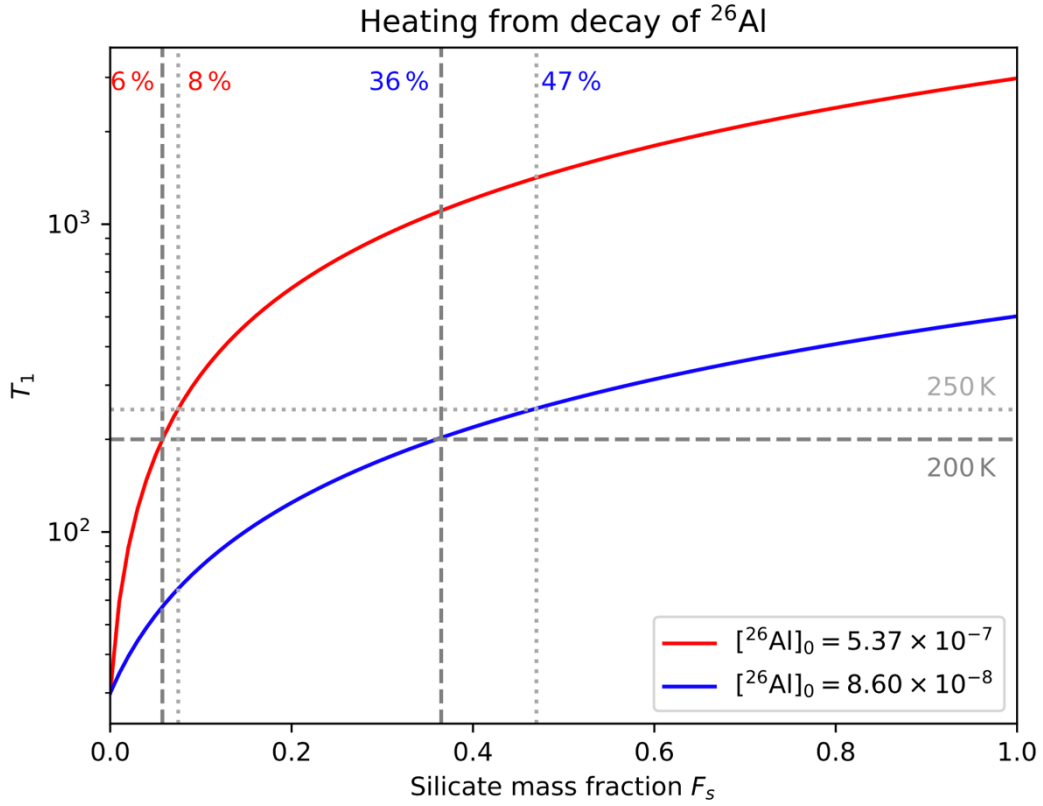

Canas & Lyra + (2024)

Integrate pebble accretion

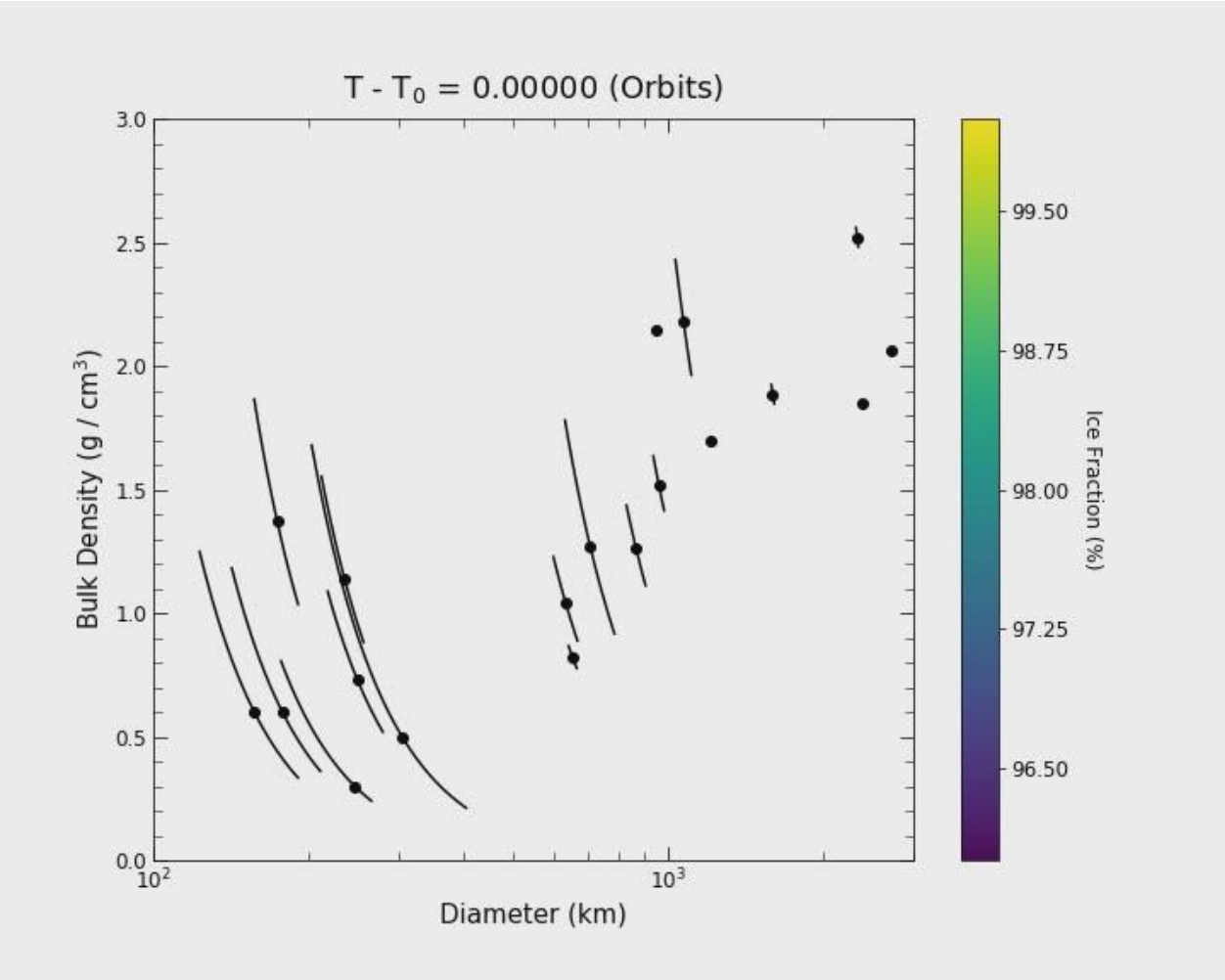

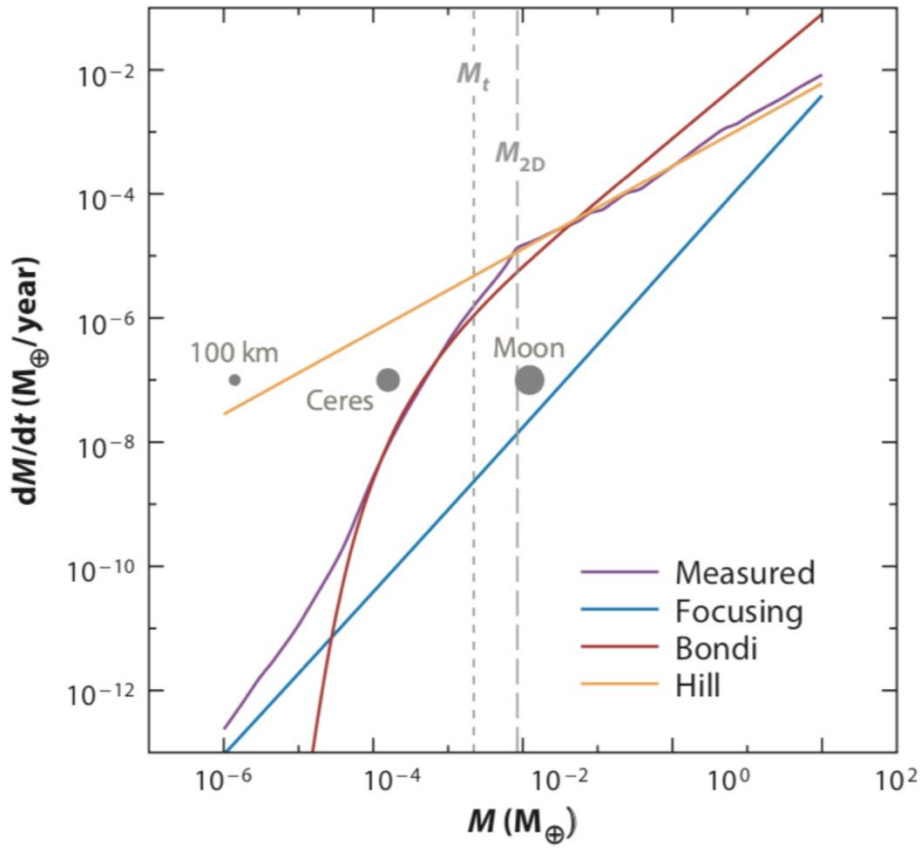

Johansen & Lambrechts (2017)

Pebble Accretion: Pebbles of different size accrete differently

Large

Medium

Small

”Goldilocks effect” in the Bondi regime

Bondi Regime

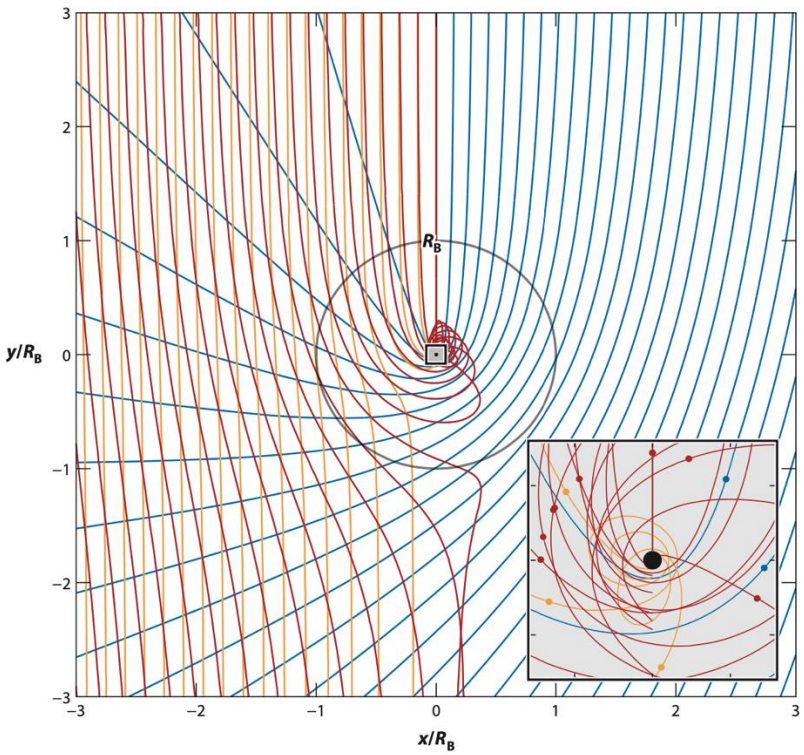

Best accreted pebble

Drag time ~ Bondi Time

Hill Regime

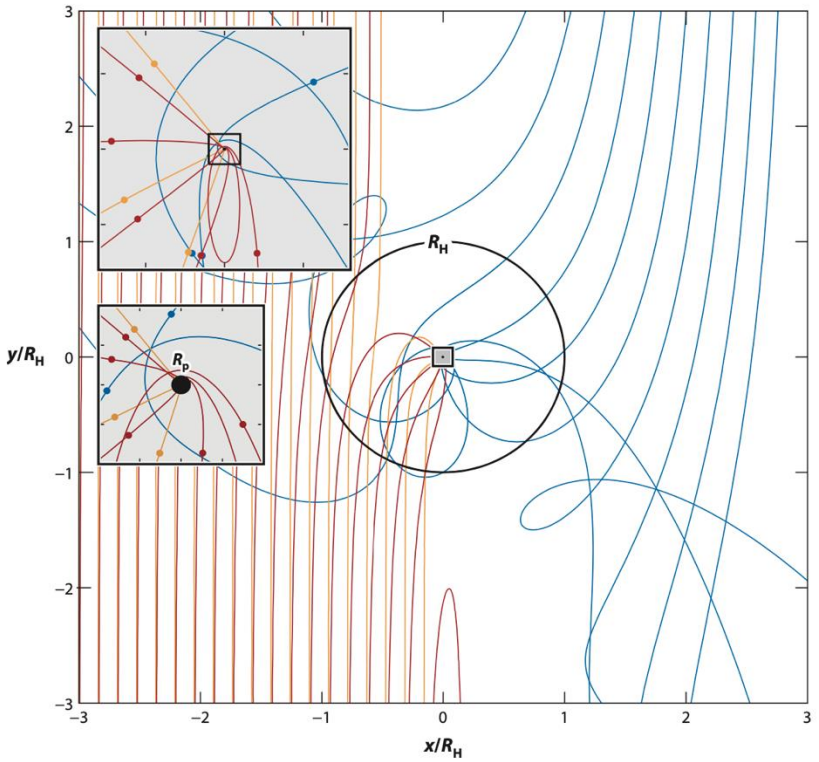

Best accreted pebble

Drag time ~ Orbital Time

Johansen & Lambrechts (2017); Lyra & Johansen + (2023)

Accretion Rates

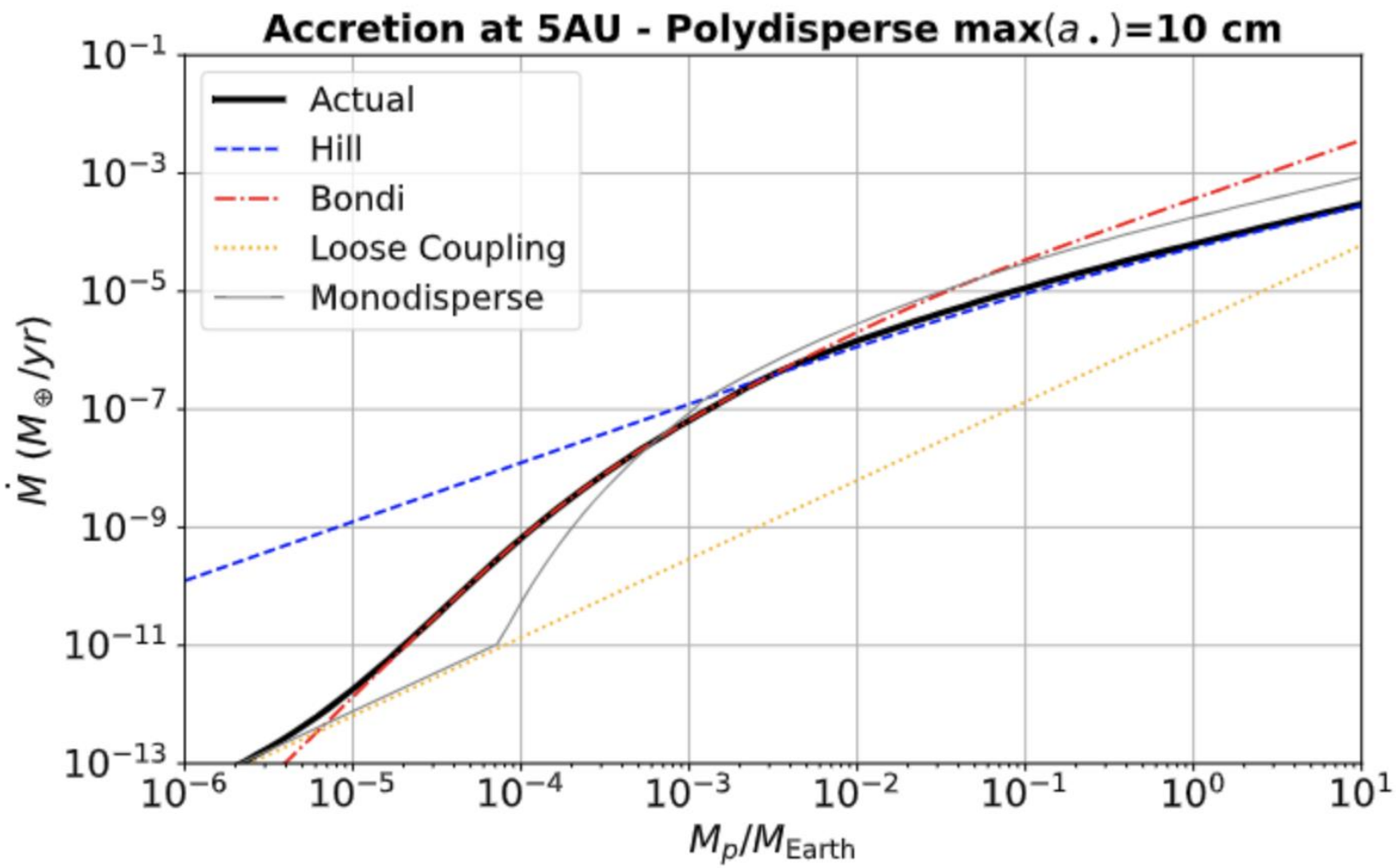

Lyra & Johansen + 2023

Differential Accretion Rates

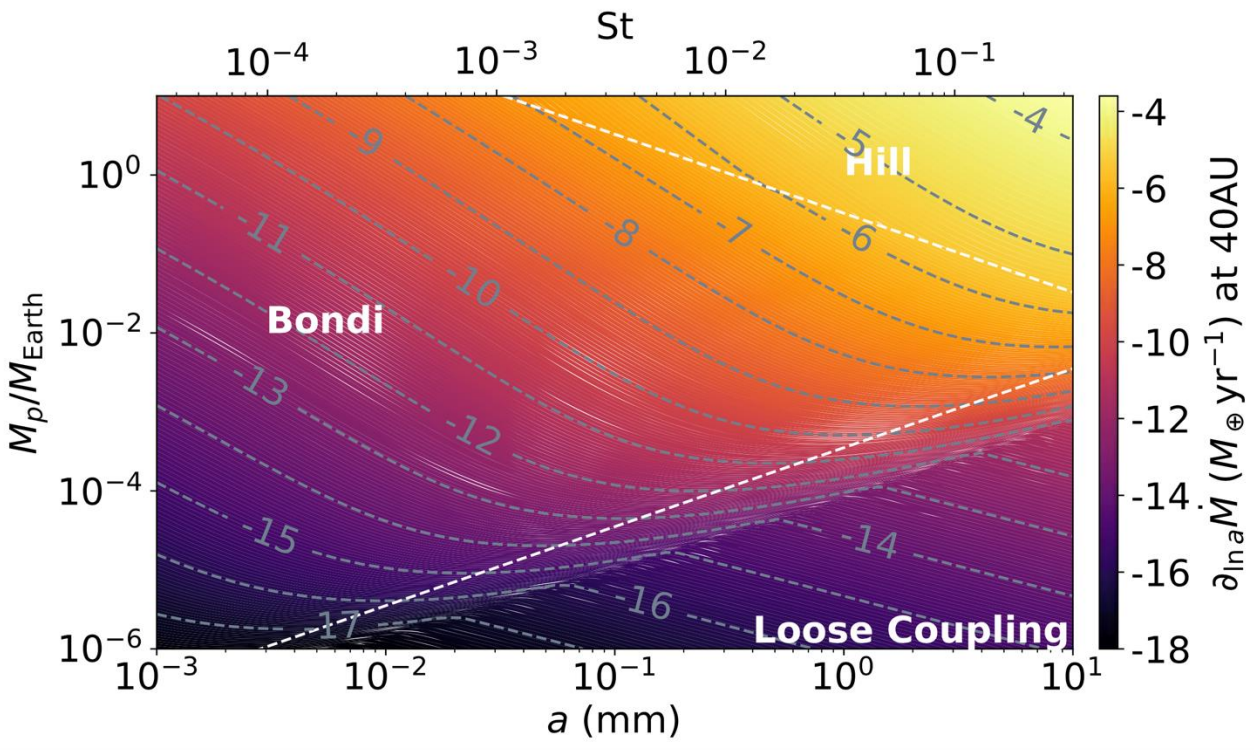

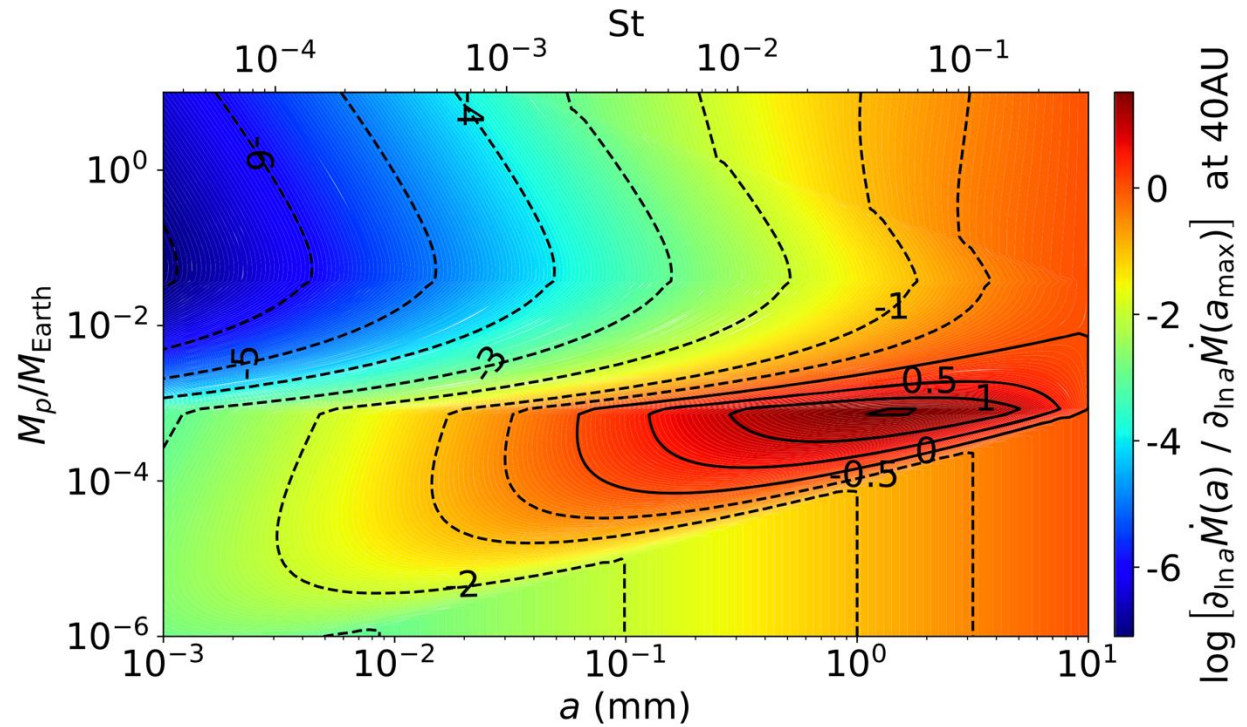

Lyra & Johansen + 2023

Accretion Timescales

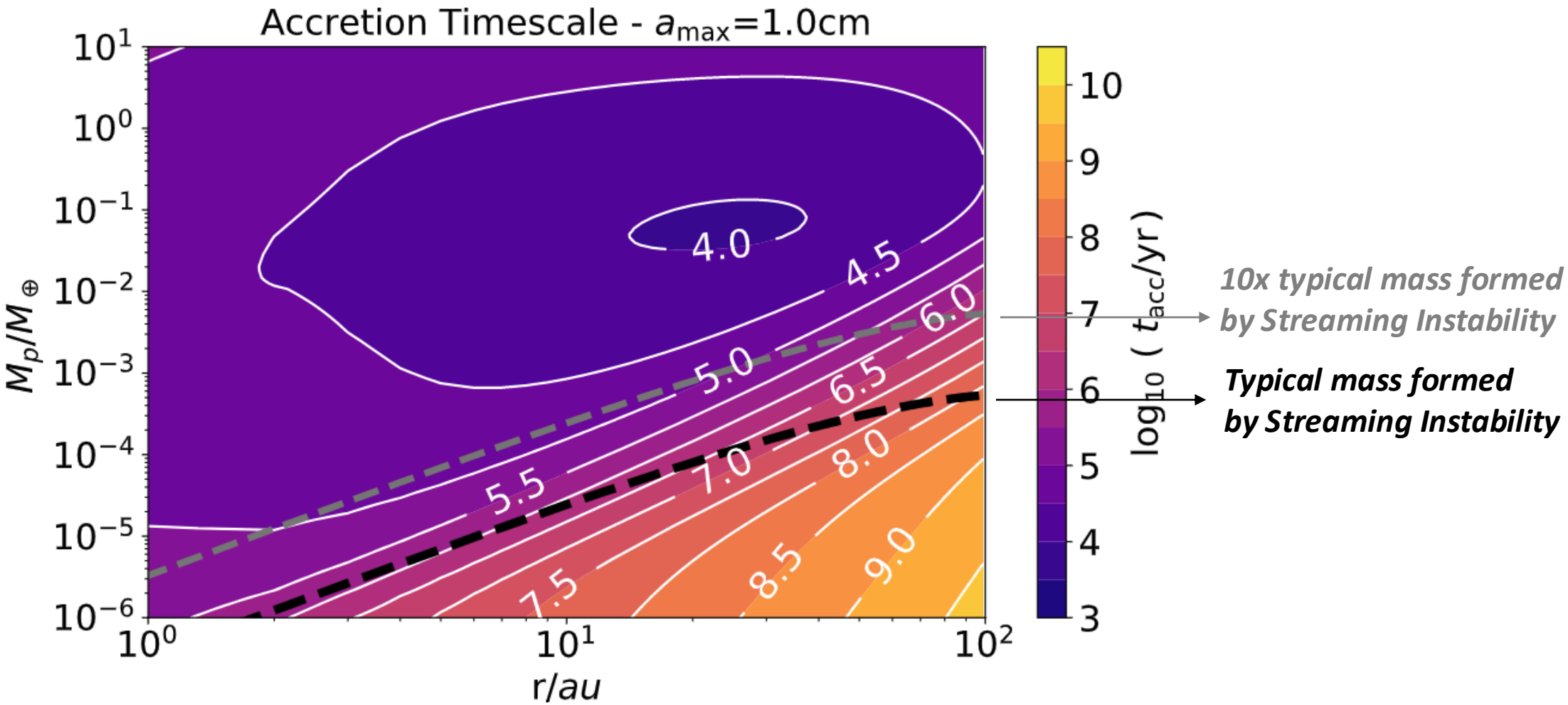

Lyra & Johansen + 2023

Polydisperse (Multi-Species) Pebble Accretion

$$\rho_d(a, z) = \int_0^a m(a')\, F(a', z)\, da'.$$

$$F(a, z) \equiv f(a)\, e^{-z^2/2H_d^2},$$

$$f(a) = \frac{3(1-p)Z\Sigma_g}{2^{5/2}\pi^{3/2}H_g\rho_\bullet^{(0)}a_{\max}^{4-k}}\sqrt{1 + a\frac{\pi}{2}\frac{\rho_\bullet(a)}{\Sigma_g\alpha}}\; a^{-k}.$$

$$\dot{M}(a) = \int_0^a \frac{\partial\dot{M}(a')}{\partial a'}da',$$

$$\frac{\partial\dot{M}(a)}{\partial a} = \pi R_{\rm acc}^2(a)\,\delta v(a)\,S(a)\,m(a)\,f(a).$$

$$S \equiv \frac{1}{\pi R_{\rm acc}^2}\int_{-R_{\rm acc}}^{R_{\rm acc}} 2\sqrt{R_{\rm acc}^2 - z^2}\,\exp\left(-\frac{z^2}{2H_d^2}\right)dz,$$

$$W(a) = \frac{3(1-p)Z\Sigma_g}{4\pi\rho_\bullet^{(0)}a_{\max}^{4-k}}\,a^{-k},$$

$$\delta v \equiv \Delta v + \Omega R_{\rm acc},$$

$$R_{\rm acc} \equiv \hat{R}_{\rm acc}\exp\left[-\chi(\tau_f/t_p)^\gamma\right],$$

$$\hat{R}_{\rm acc}^{\rm (Bondi)} = \left(\frac{4\tau_f}{t_{\rm B}}\right)^{1/2}R_{\rm B},$$

$$\hat{R}_{\rm acc}^{\rm (Hill)} = \left(\frac{\rm St}{0.1}\right)^{1/3}R_{\rm H},$$

$$\frac{\partial\Sigma_d(a)}{\partial a} \propto a^{-p};$$

$$\rho_\bullet \propto a^{-q};$$

$$t_p \equiv \frac{GM_p}{(\Delta v + \Omega R_{\rm H})^3}$$

$$\dot{M}_{\rm 2D,\ Hill} = 2\times 10^{2/3}\Omega R_H^2\int_0^{a_{\max}} {\rm St}(a)^{2/3}\, m(a)\, W(a)\, da.$$

$$\dot{M}_{\rm 3D,\ Bondi} = \frac{4\pi R_{\rm B}\Delta v^2}{\Omega} \times \int_0^{a_{\max}} {\rm St}\; e^{-2\psi}m(a)f(a) \times\left[1 + 2\left({\rm St}\frac{\Omega R_{\rm B}}{\Delta v}\right)^{1/2}e^{-\psi}\right]da, \qquad \psi \equiv \chi[{\rm St}/(\Omega t_p)]^\gamma.$$

Lyra & Johansen + 2023

Analytical theory of polydisperse (multi-species) pebble accretion

$\xi \equiv \left(\frac{R_{\rm acc}}{2H_d}\right)^2$

Monodisperse (single species)

$$\dot{M}_{\rm 3D} = \lim_{\xi \to 0} \dot{M} = \pi R_{\rm acc}^2 \rho_{d0} \delta v,$$

$$\dot{M}_{\rm 2D} = \lim_{\xi \to \infty} \dot{M} = 2 R_{\rm acc} \Sigma_d \delta v,$$

Lambrechts & Johansen (2012)

Polydisperse (multiple species)

$$\dot{M}_{\rm 2D,Hill} = \frac{6(1-p)}{14-5q-3k} \left(\frac{\rm St_{max}}{0.1}\right)^{2/3} \Omega R_H^2 Z \Sigma_g$$

$$\dot{M}_{\rm 3D,Bondi} \approx C_1 \frac{\gamma_l\left(\frac{b_1+1}{s}, j_1 a_{\rm max}^s\right)}{s j_1^{(b_1+1)/s}} + C_2 \frac{\gamma_l\left(\frac{b_2+1}{s}, j_2 a_{\rm max}^s\right)}{s j_2^{(b_2+1)/s}} + C_3 \frac{\gamma_l\left(\frac{b_3+1}{s}, j_3 a_{\rm max}^s\right)}{s j_3^{(b_3+1)/s}} + C_4 \frac{\gamma_l\left(\frac{b_4+1}{s}, j_4 a_{\rm max}^s\right)}{s j_4^{(b_4+1)/s}},$$

Lyra et al. (2023)

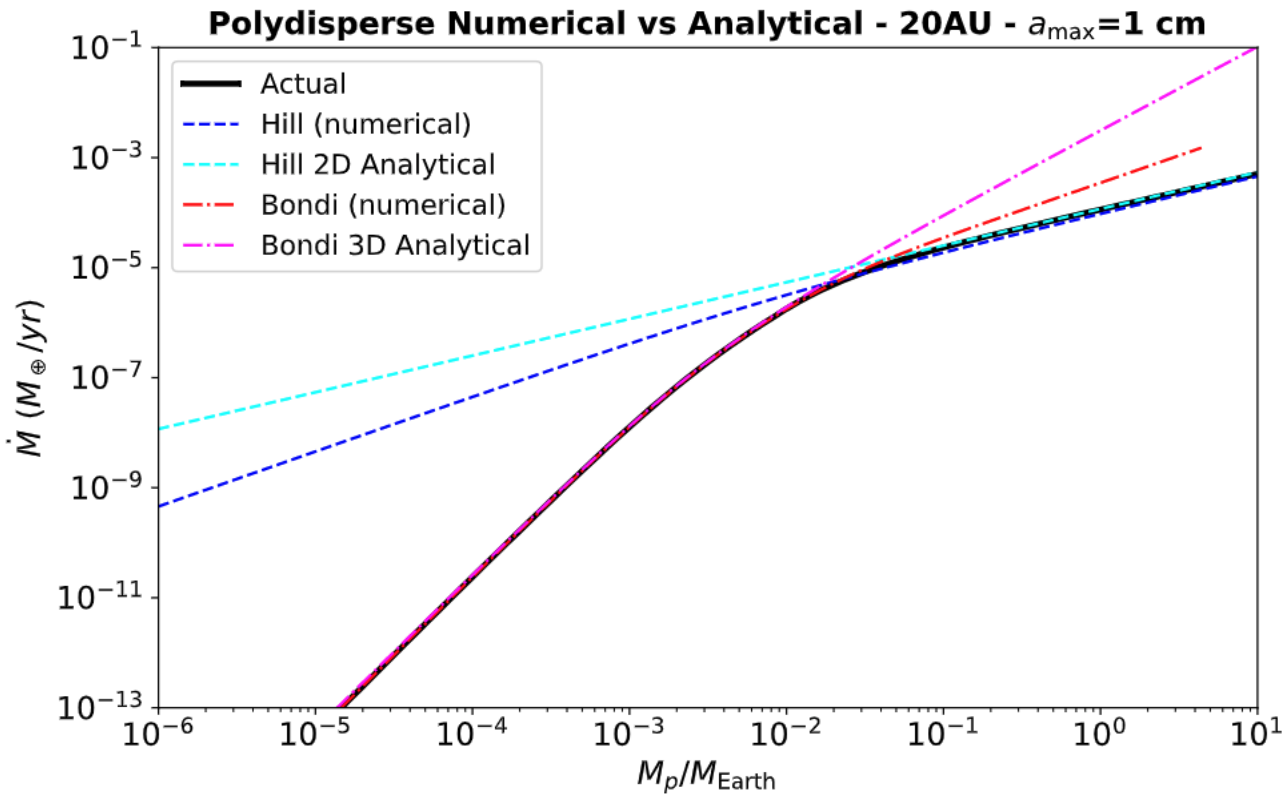

Lyra & Johansen + 2023

Analytical Solutions

$$\dot{M} = \pi R_{\rm acc}^2 \rho_{d0}\, S\, \delta v.$$

$$S \equiv \frac{1}{\pi R_{\rm acc}^2} \int_{-R_{\rm acc}}^{R_{\rm acc}} 2\sqrt{R_{\rm acc}^2 - z^2}\, \exp\left(-\frac{z^2}{2H_d^2}\right)\, dz,$$

$$S = e^{-\xi}\,[I_0(\xi) + I_1(\xi)], \qquad \xi \equiv \left(\frac{R_{\rm acc}}{2H_d}\right)^2$$

```
y = (x/2)**2

# Modified Bessel function of the first kind of real order.
I0 = sp.special.iv(0, y)
I1 = sp.special.iv(1, y)

Sint = np.exp(-y) * (I0 + I1)
rho_int = rhop * Sint
Mdot = pi*r**2 * rho_int * deltav
```

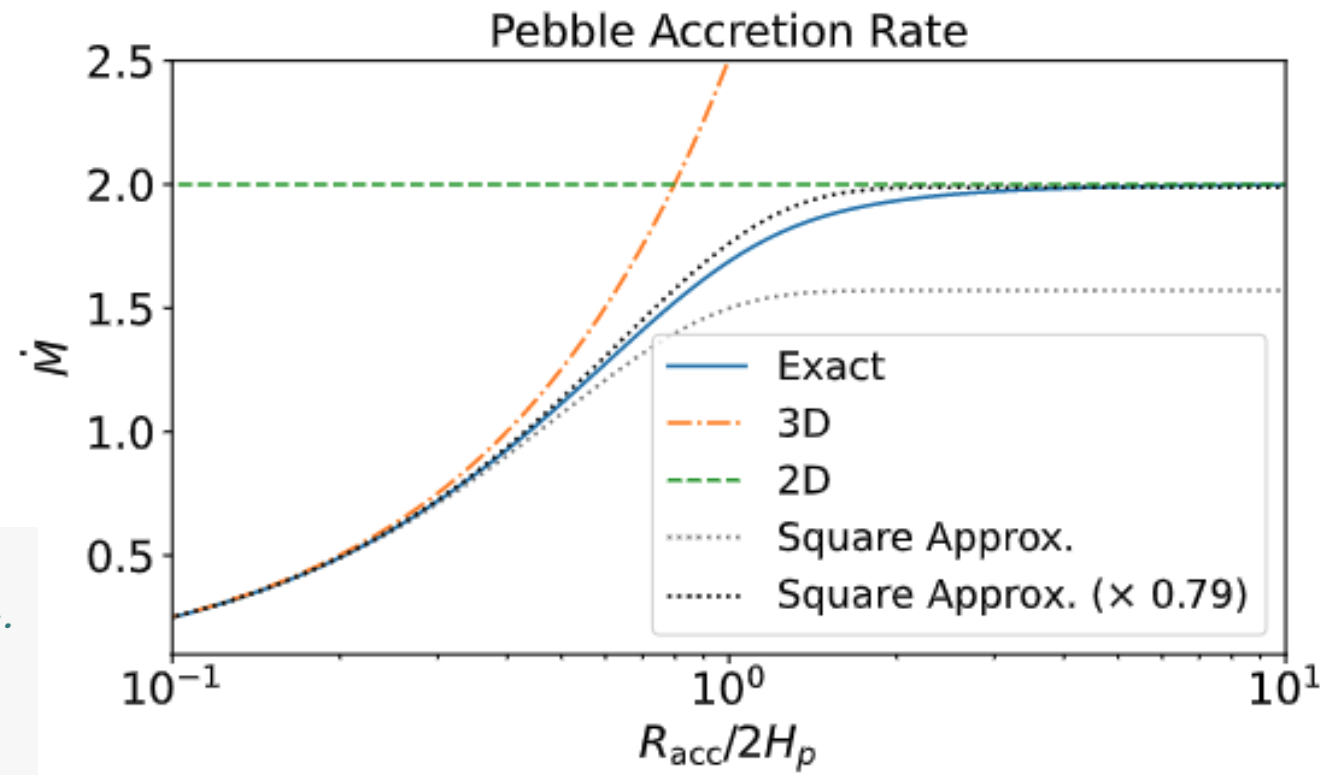

Lyra et al. 2023

Analytical Solutions

$$\dot{M}_{\rm 2D,Hill} = \frac{6(1-p)}{14-5q-3k}\left(\frac{\rm St_{max}}{0.1}\right)^{2/3} \Omega R_H^2 Z \Sigma_g$$

$$\dot{M}_{\rm 3D,Bondi} \approx C_1 \frac{\gamma_l\left(\frac{b_1+1}{s}, j_1 a_{\rm max}^s\right)}{s j_1^{(b_1+1)/s}} + C_2 \frac{\gamma_l\left(\frac{b_2+1}{s}, j_2 a_{\rm max}^s\right)}{s j_2^{(b_2+1)/s}} + C_3 \frac{\gamma_l\left(\frac{b_3+1}{s}, j_3 a_{\rm max}^s\right)}{s j_3^{(b_3+1)/s}} + C_4 \frac{\gamma_l\left(\frac{b_4+1}{s}, j_4 a_{\rm max}^s\right)}{s j_4^{(b_4+1)/s}}$$

```
gamma1 = sp.special.gammainc((b1+1)/s,j1*a**s)*sp.special.gamma((b1+1)/s)
gamma2 = sp.special.gammainc((b2+1)/s,j2*a**s)*sp.special.gamma((b2+1)/s)
gamma3 = sp.special.gammainc((b3+1)/s,j3*a**s)*sp.special.gamma((b3+1)/s)
gamma4 = sp.special.gammainc((b4+1)/s,j4*a**s)*sp.special.gamma((b4+1)/s)

G1 = C1*gamma1/s/j1**((b1+1)/s)
G2 = C2*gamma2/s/j2**((b2+1)/s)
G3 = C3*gamma3/s/j3**((b3+1)/s)
G4 = C4*gamma4/s/j4**((b4+1)/s)

Mbondi3d = G1 + G2 + G3 + G4
```

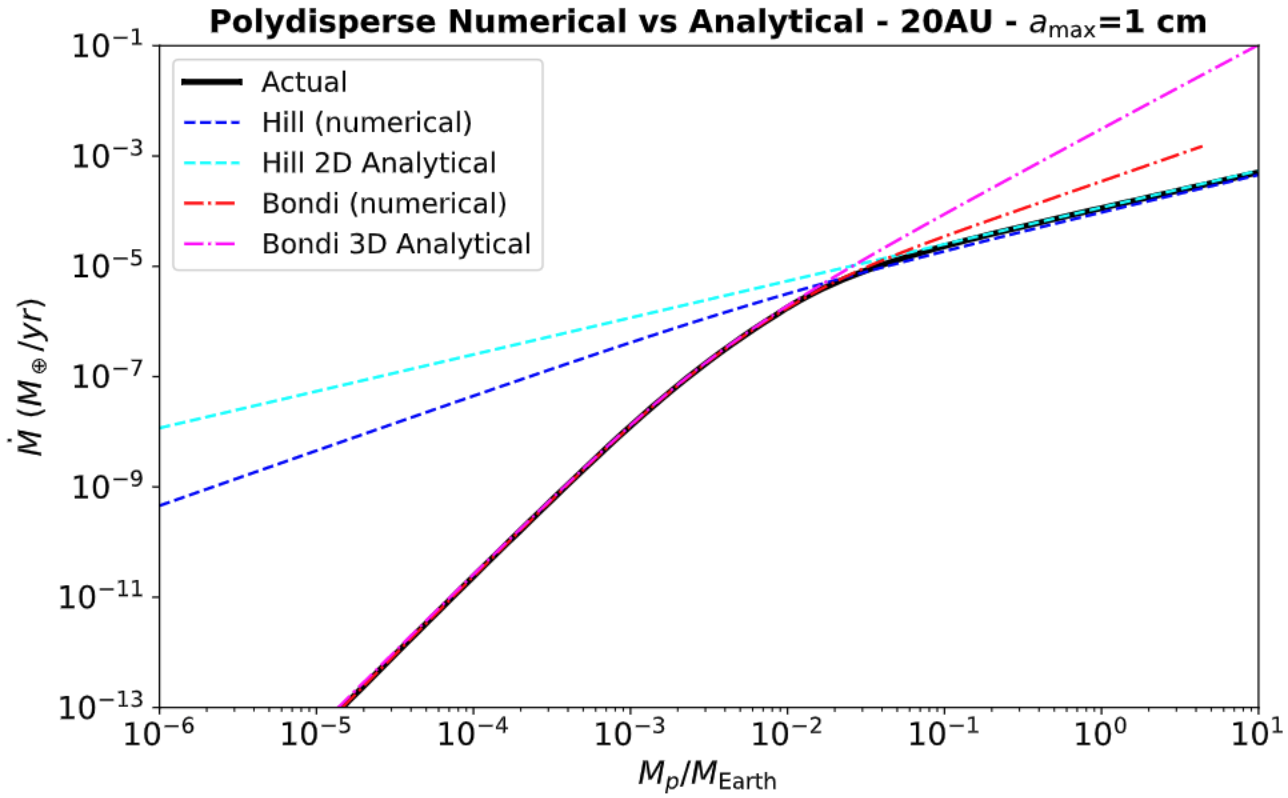

Lyra et al. 2023

Growing Pluto by silicate pebble accretion

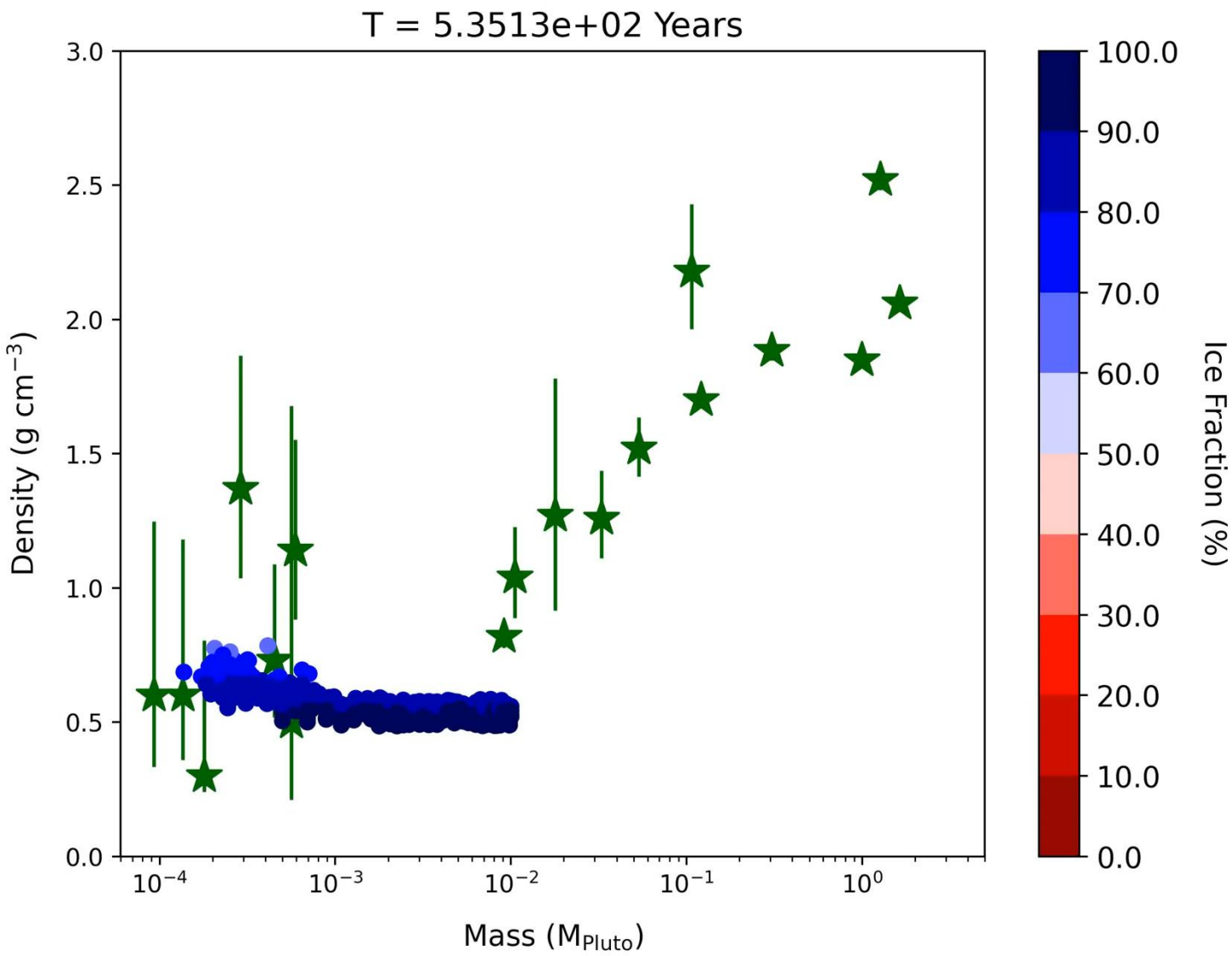

Canas & Lyra + (2024)

Pebble Internal Density

Ice Volume Fraction

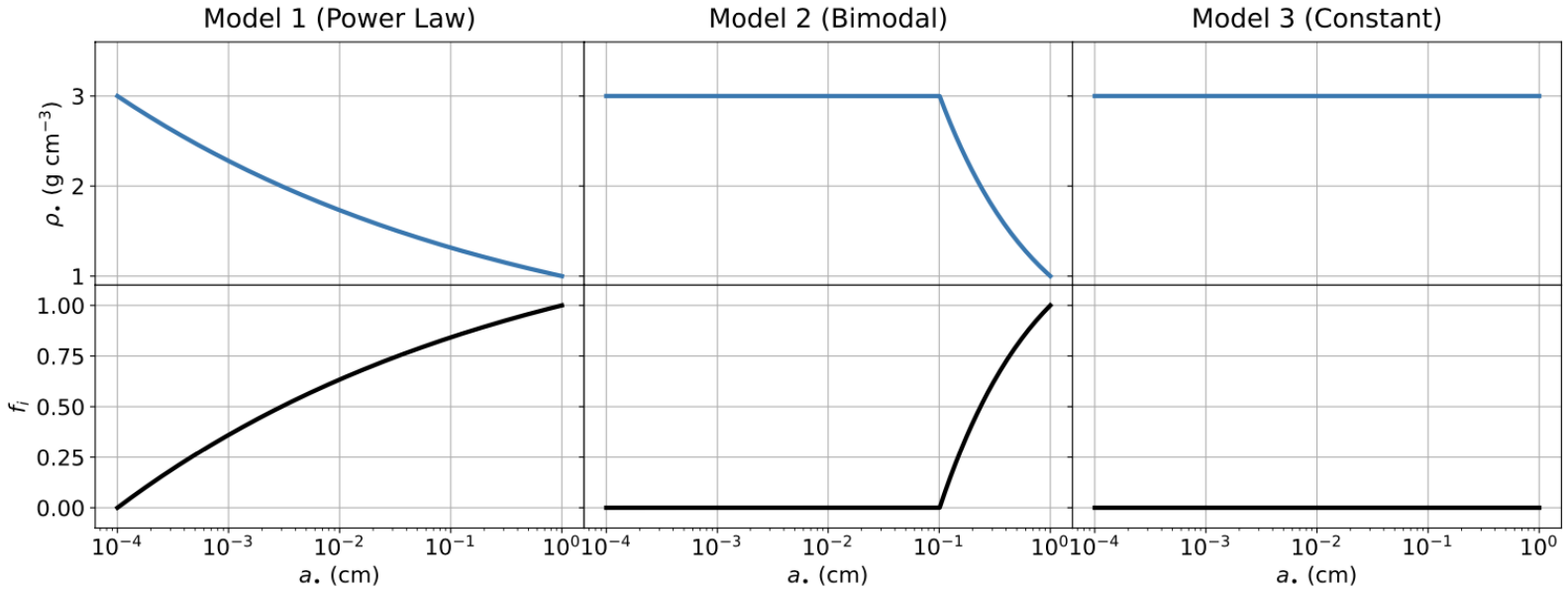

Mass Accretion rate

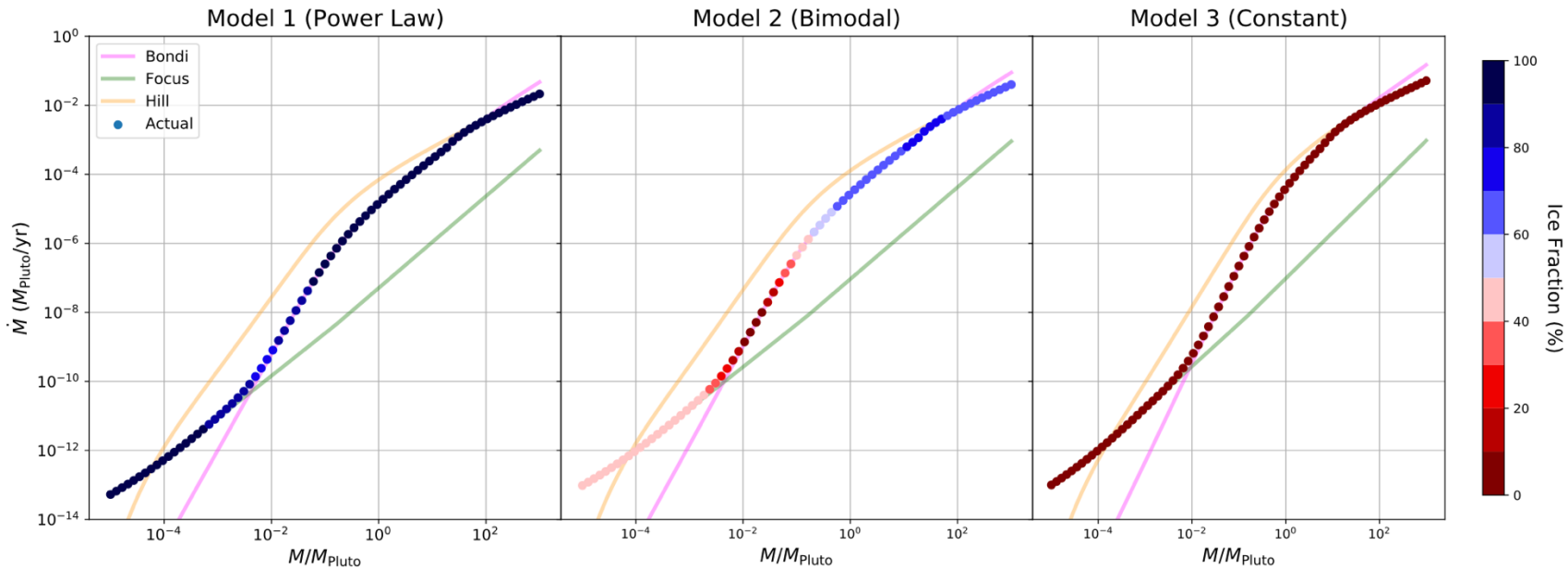

Canas & Lyra + (2024)

Growing Pluto by silicate pebble accretion

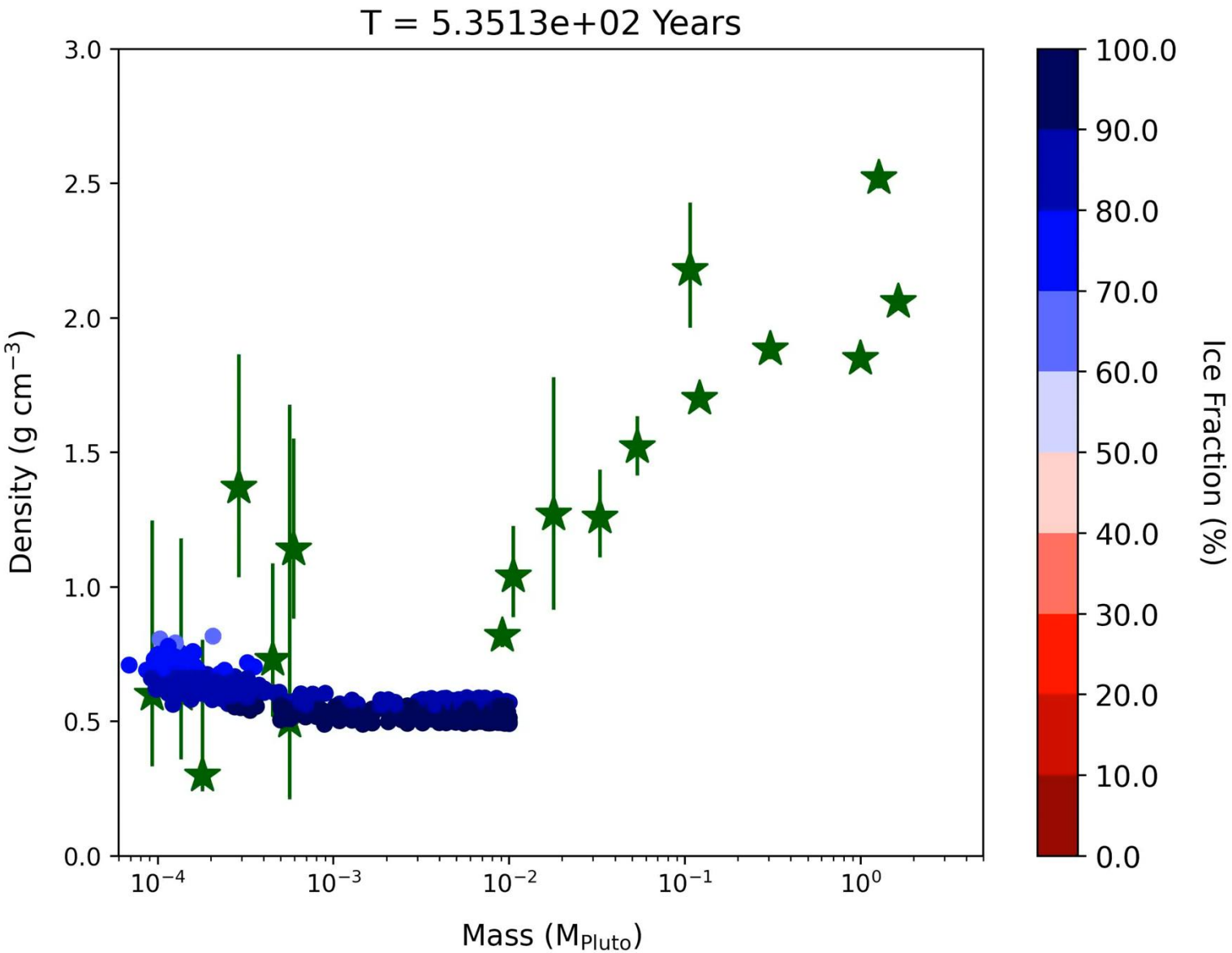

Canas & Lyra + (2024)

Resulting Densities vs Mass relations

Pebble Internal Density

Ice Volume Fraction

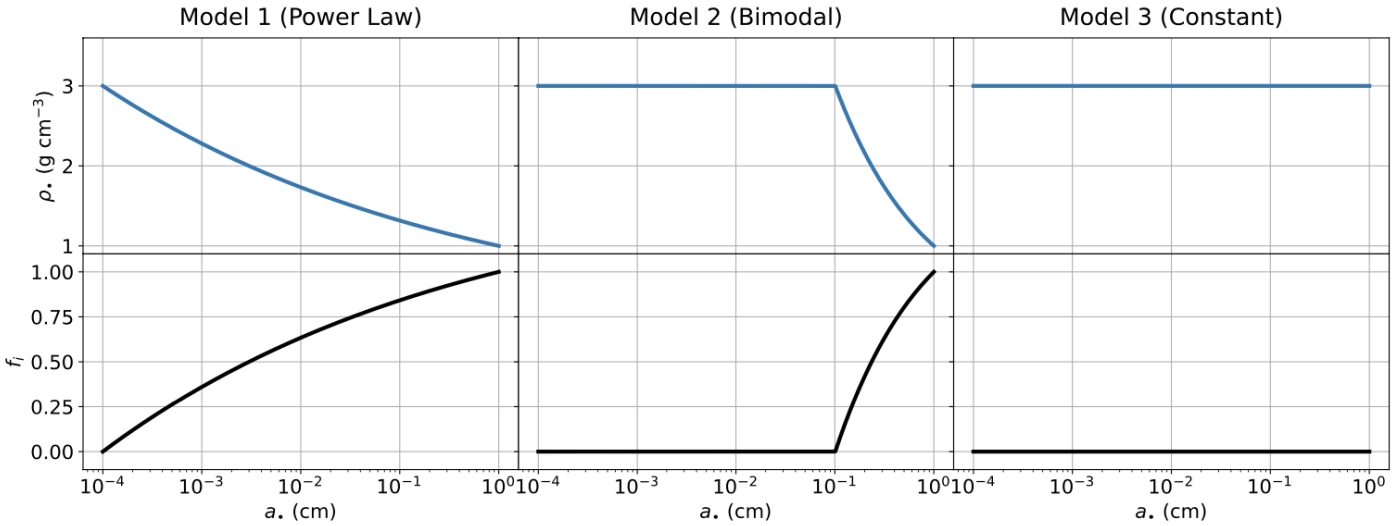

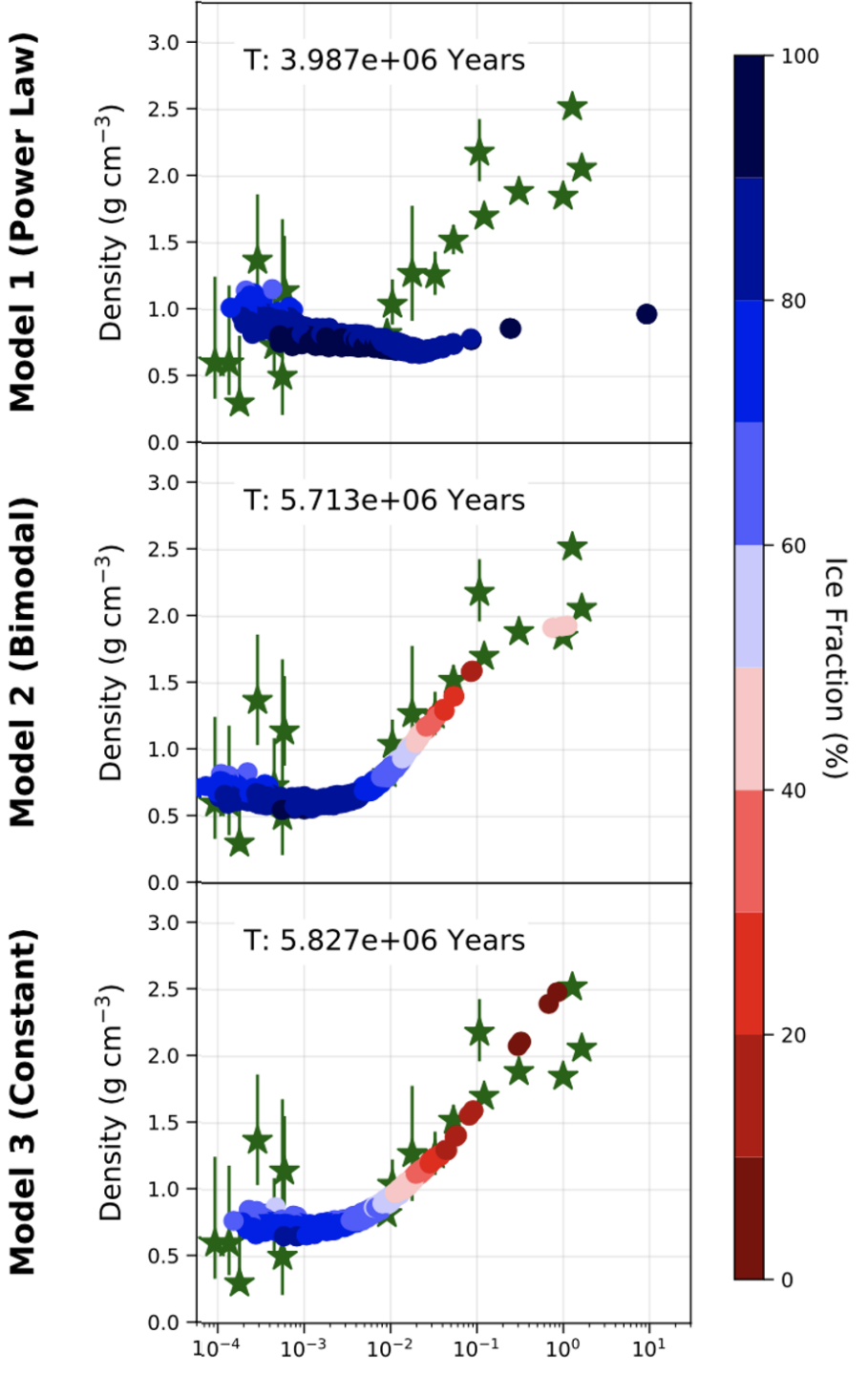

Canas & Lyra + (2024)

Distance Range
15 - 25AU

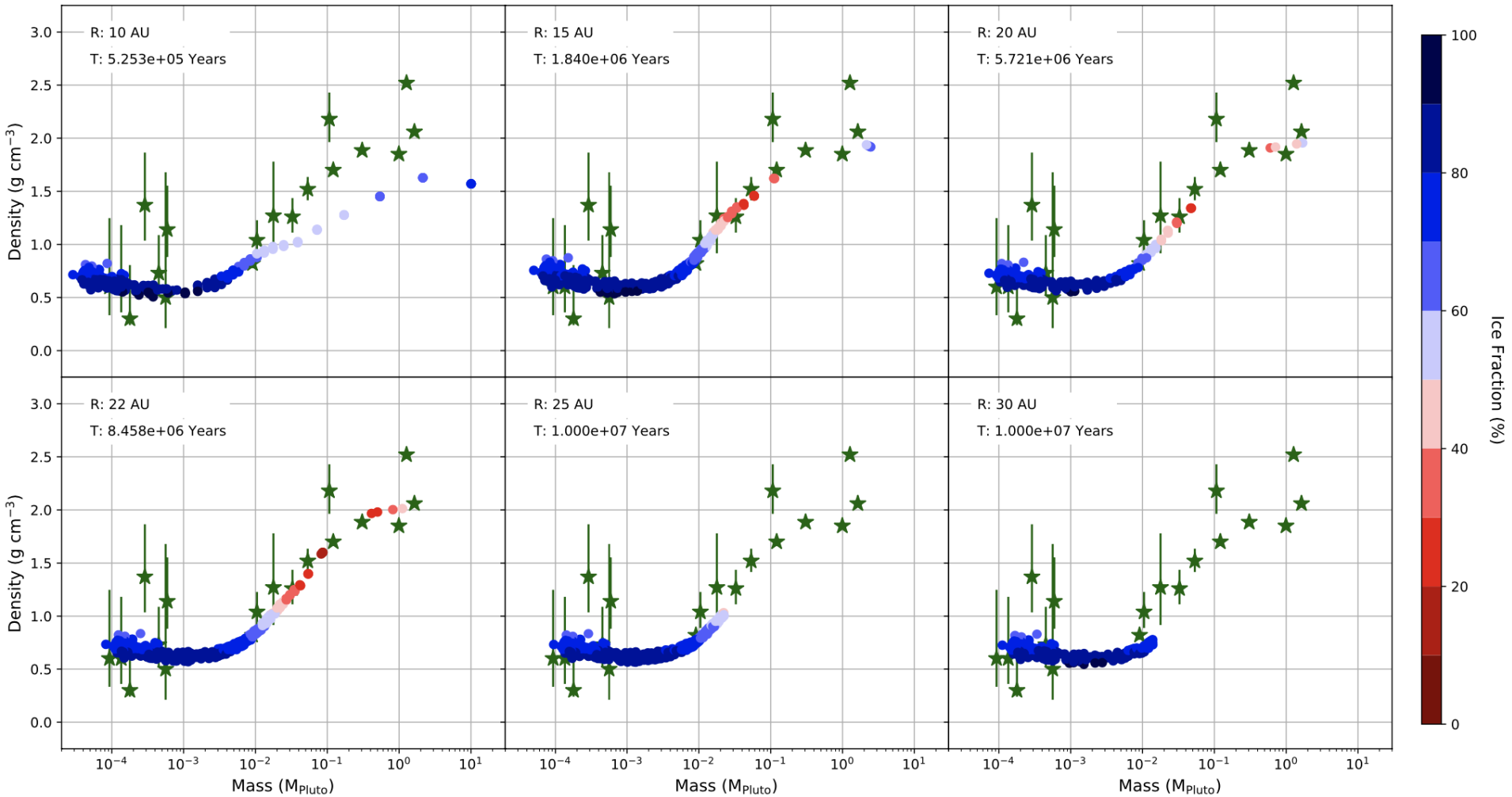

Canas & Lyra + (2024)

The window of silicate accretion

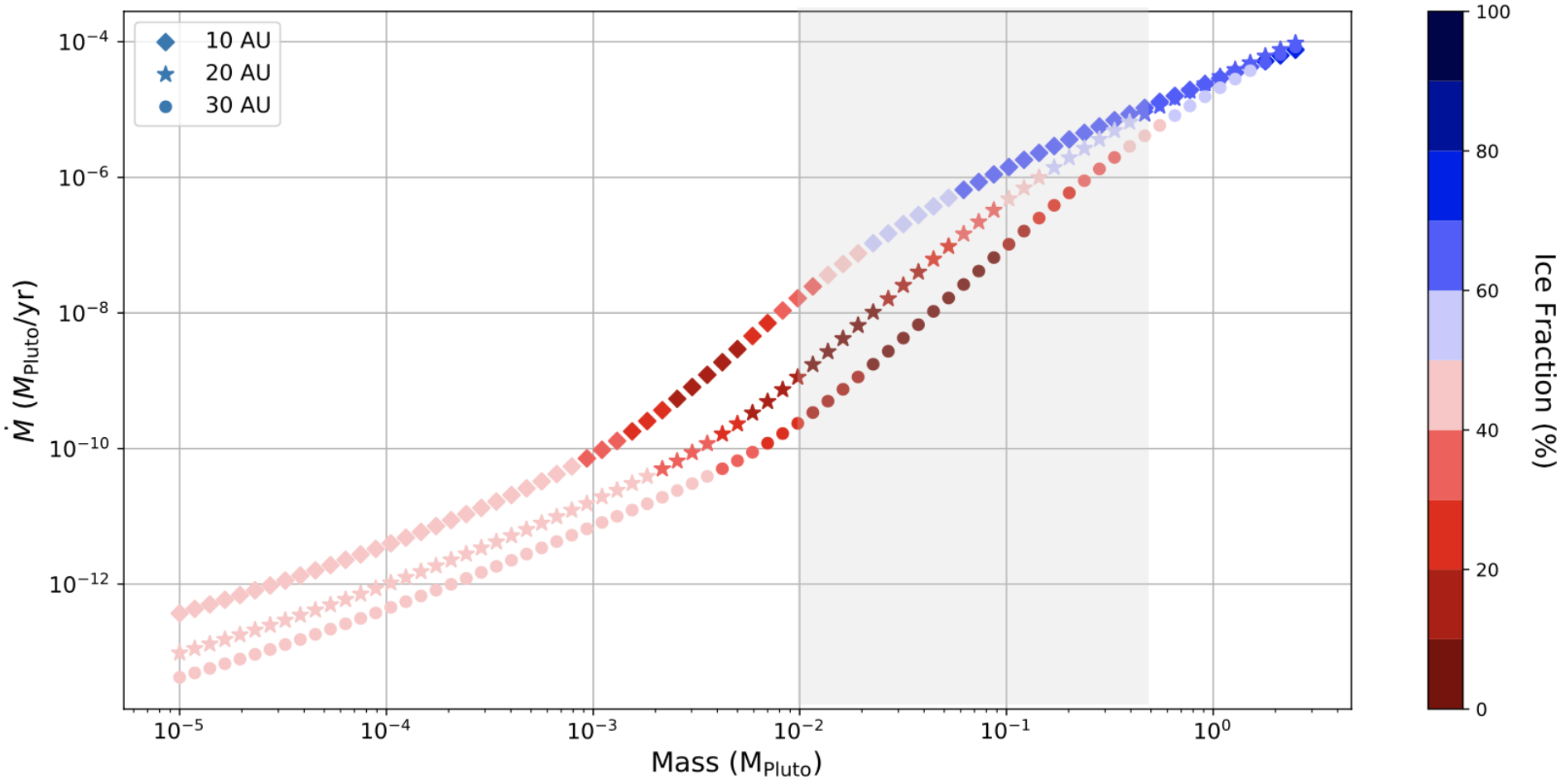

Canas & Lyra + (2024)

Where are the missing Kuiper Belt binaries?

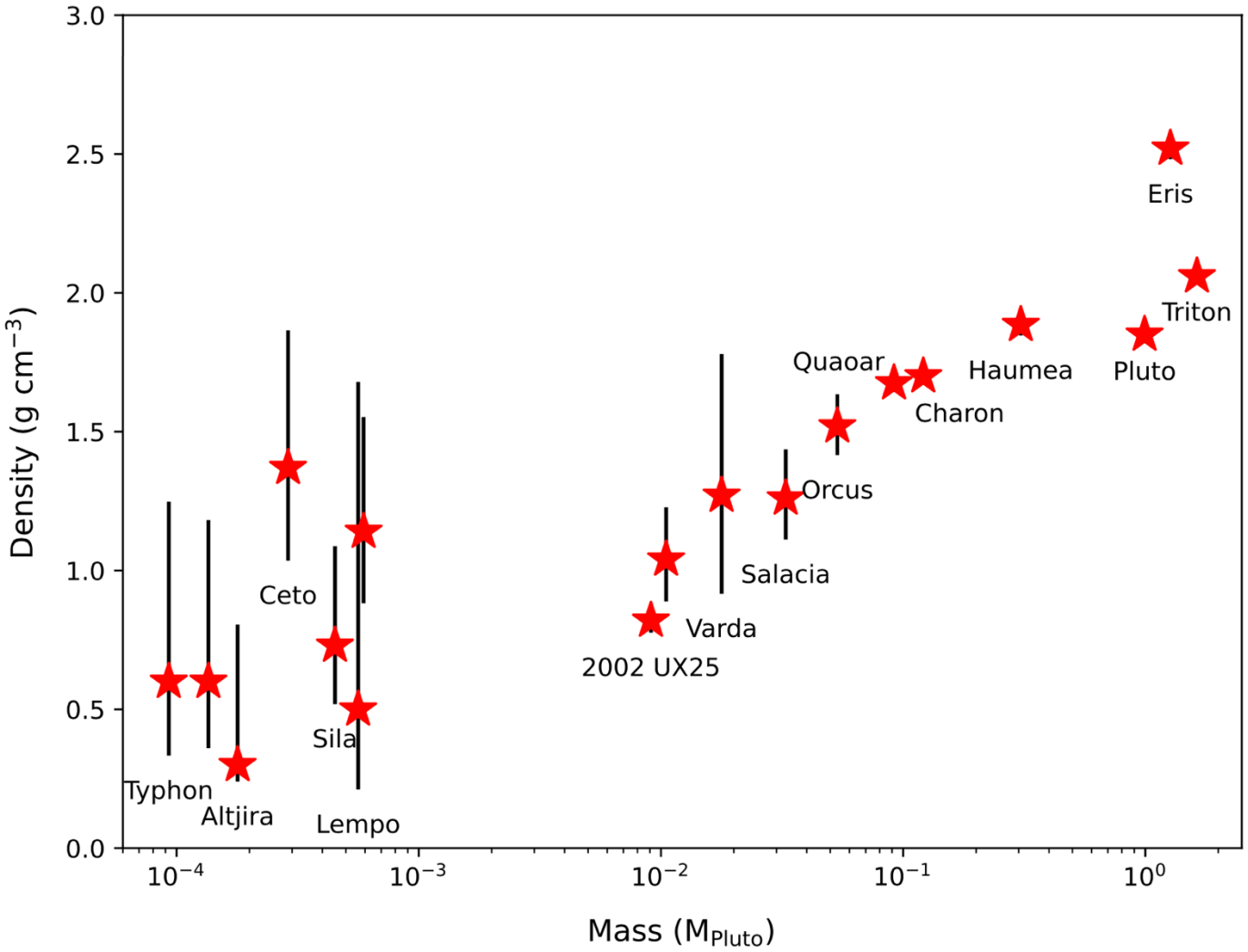

Lyra (2025)

Mass gap

Brown 2013

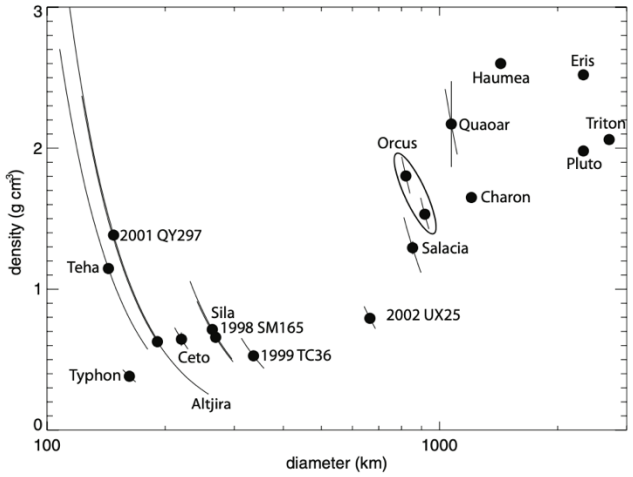

Grundy et al. 2015

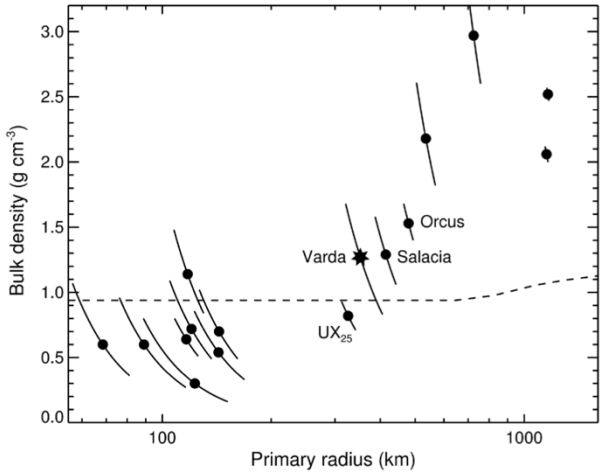

McKinnon et al. 2017

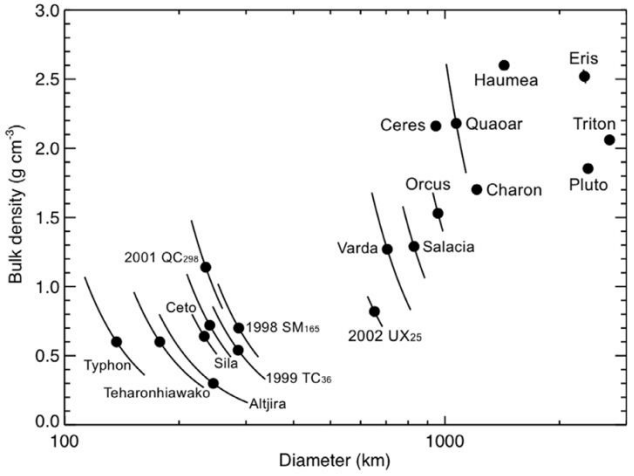

Bierson & Nimmo 2019

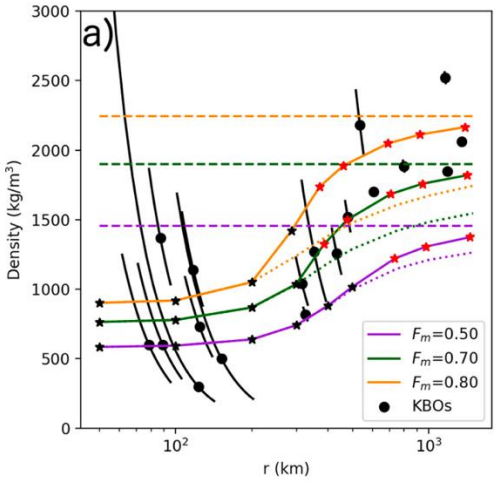

Noll et al. 2020

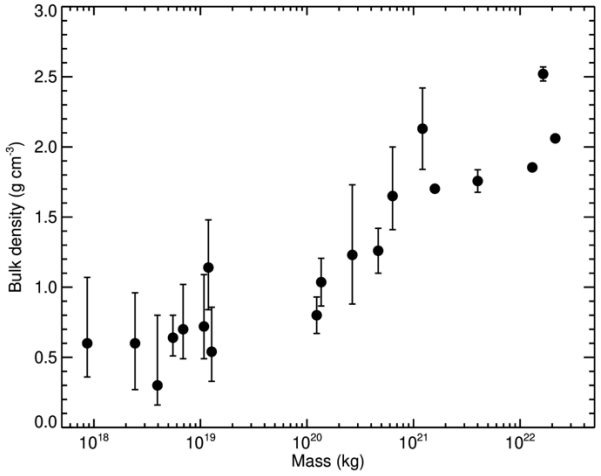

Canas et al. 2024

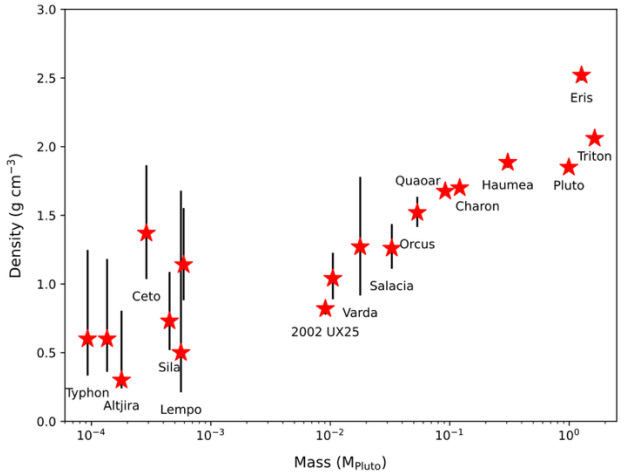

Rommel et al. 2025

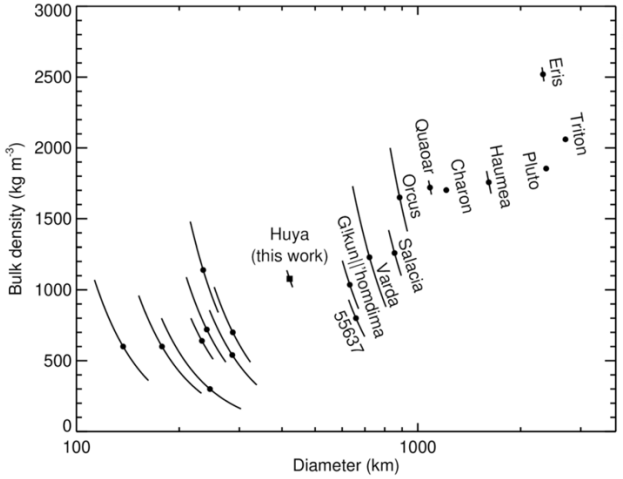

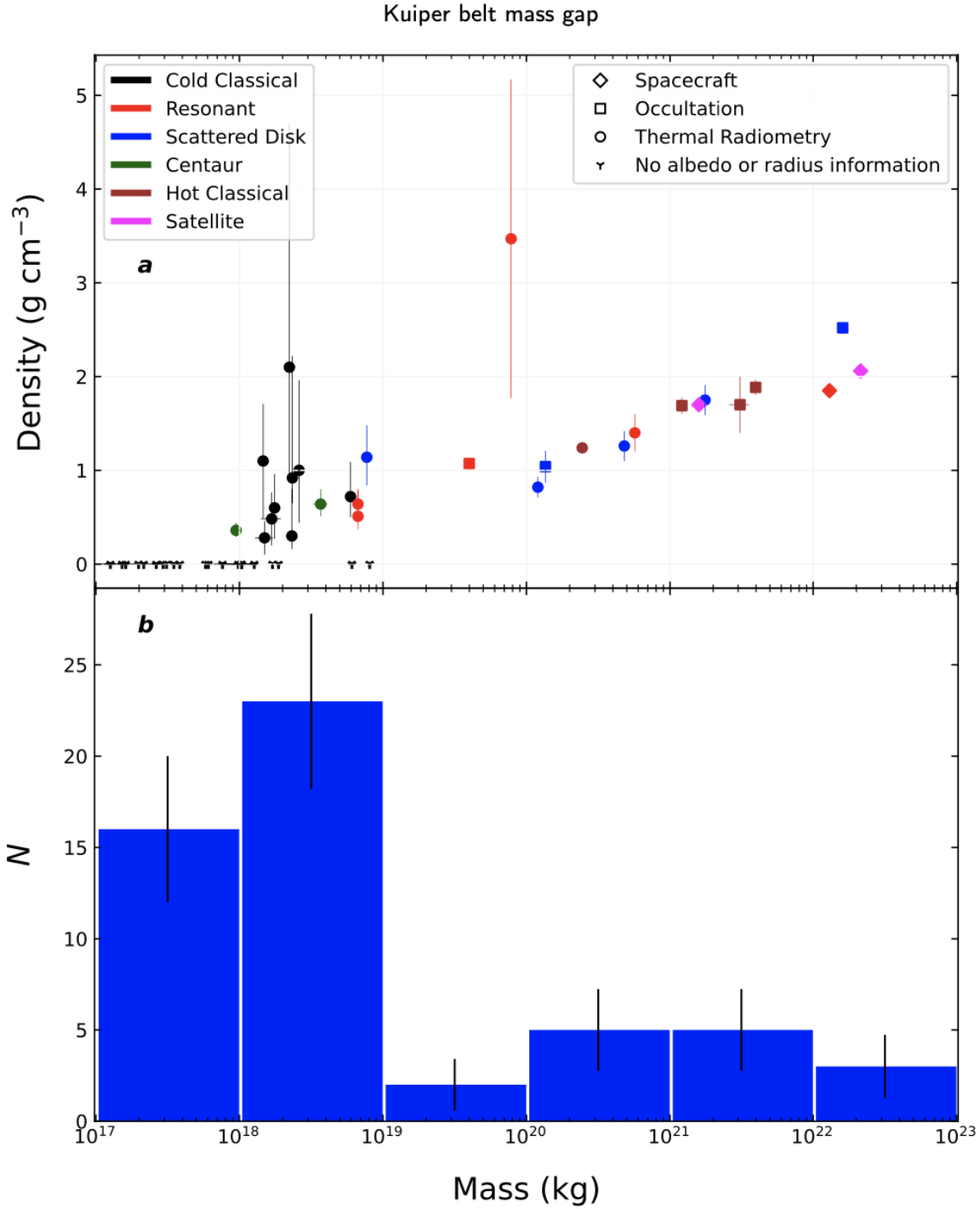

Where are the missing Kuiper Belt binaries?

- Gap between 10^{19} and 10^{20} kg (10^{-3} and 10^{-2} Pluto masses)
- Population difference
  - Cold Classicals are on low-mass side of the gap
- Likely not small number statistics
- *Low mass side is the high-mass end of the planetesimal initial mass function.*

Lyra (2025)

Low-mass end: consistent with high-mass end of Streaming Instability

A&A 597, A69 (2017)
DOI: 10.1051/0004-6361/201629561

Astronomy & Astrophysics

Initial mass function of planetesimals formed by the streaming instability

Urs Schäfer[1,2], Chao-Chin Yang[2], and Anders Johansen[2]

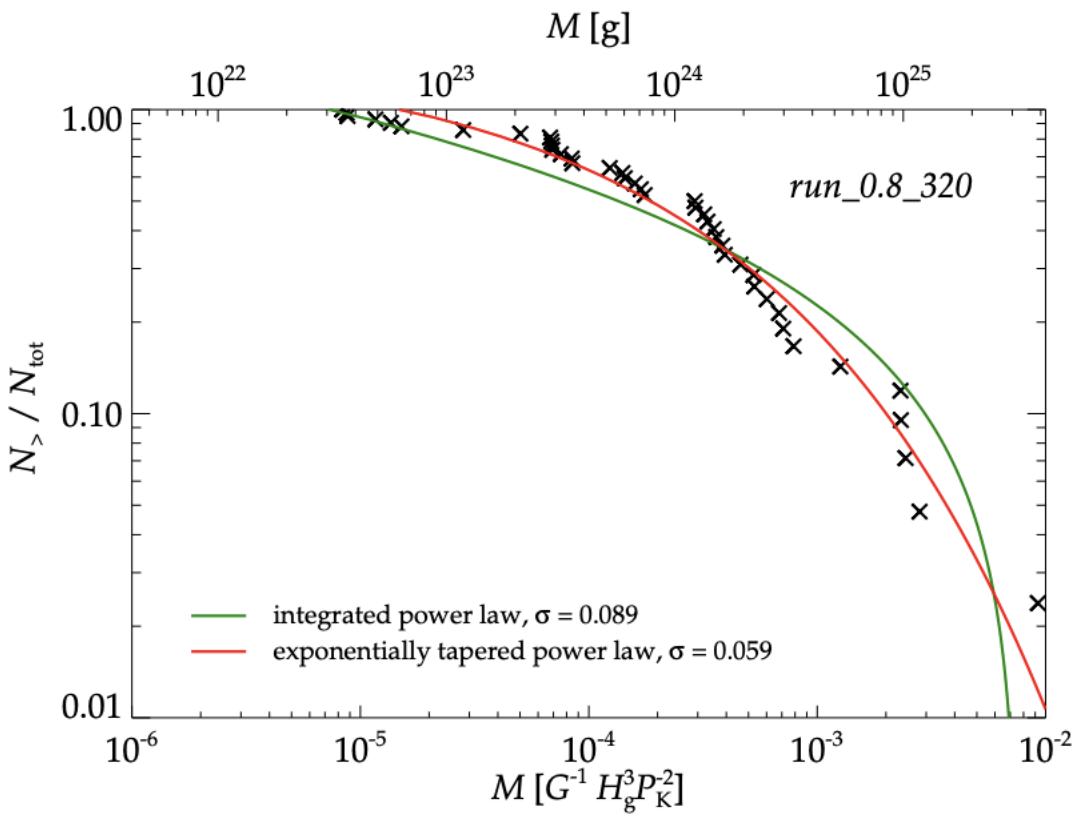

Schafer et al. (2017)

The Planetary Science Journal, 5:50 (18pp), 2024 February
https://doi.org/10.3847/PSJ/ad1528

The DECam Ecliptic Exploration Project (DEEP). V. The Absolute Magnitude Distribution of the Cold Classical Kuiper Belt

Kevin J. Napier[1], Hsing Wen Lin (林省文)[1], David W. Gerdes[1,2], Fred C. Adams[1,2], Anna M. Simpson[1,2], Matthew W. Porter[1], Katherine G. Weber[3], Larissa Markwardt[2], Gabriel Gowman[1,2], Hayden Smotherman[4], Pedro H. Bernardinelli[4], Mario Jurić[4], Andrew J. Connolly[4], J. Bryce Kalmbach[4], Stephen K. N. Portillo[4], David E. Trilling[5], Ryder Strauss[5], William J. Oldroyd[5], Chadwick A. Trujillo[5], Colin Orion Chandler[4,5,6], Matthew J. Holman[7], Hilke E. Schlichting[8], and Andrew McNeill[9,10]

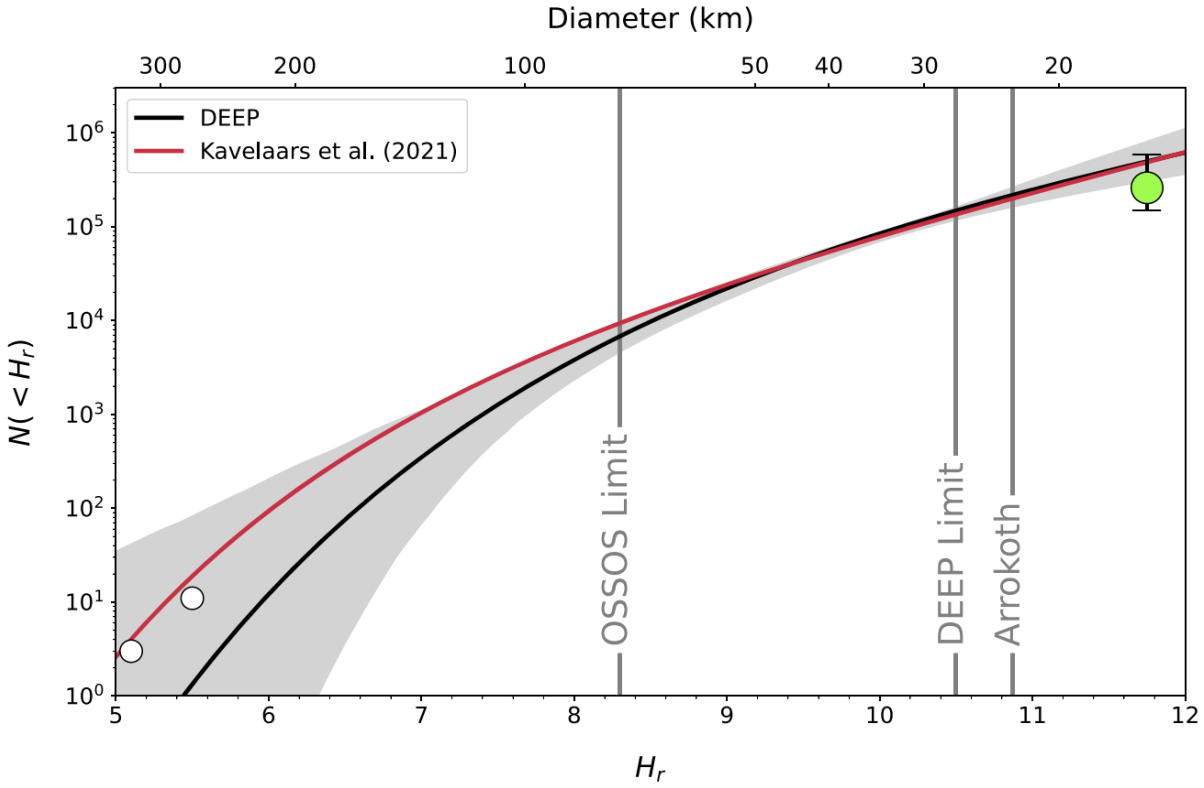

Kavelaars et al (2021); Napier et al. (2024)

High-mass side. Observational bias?

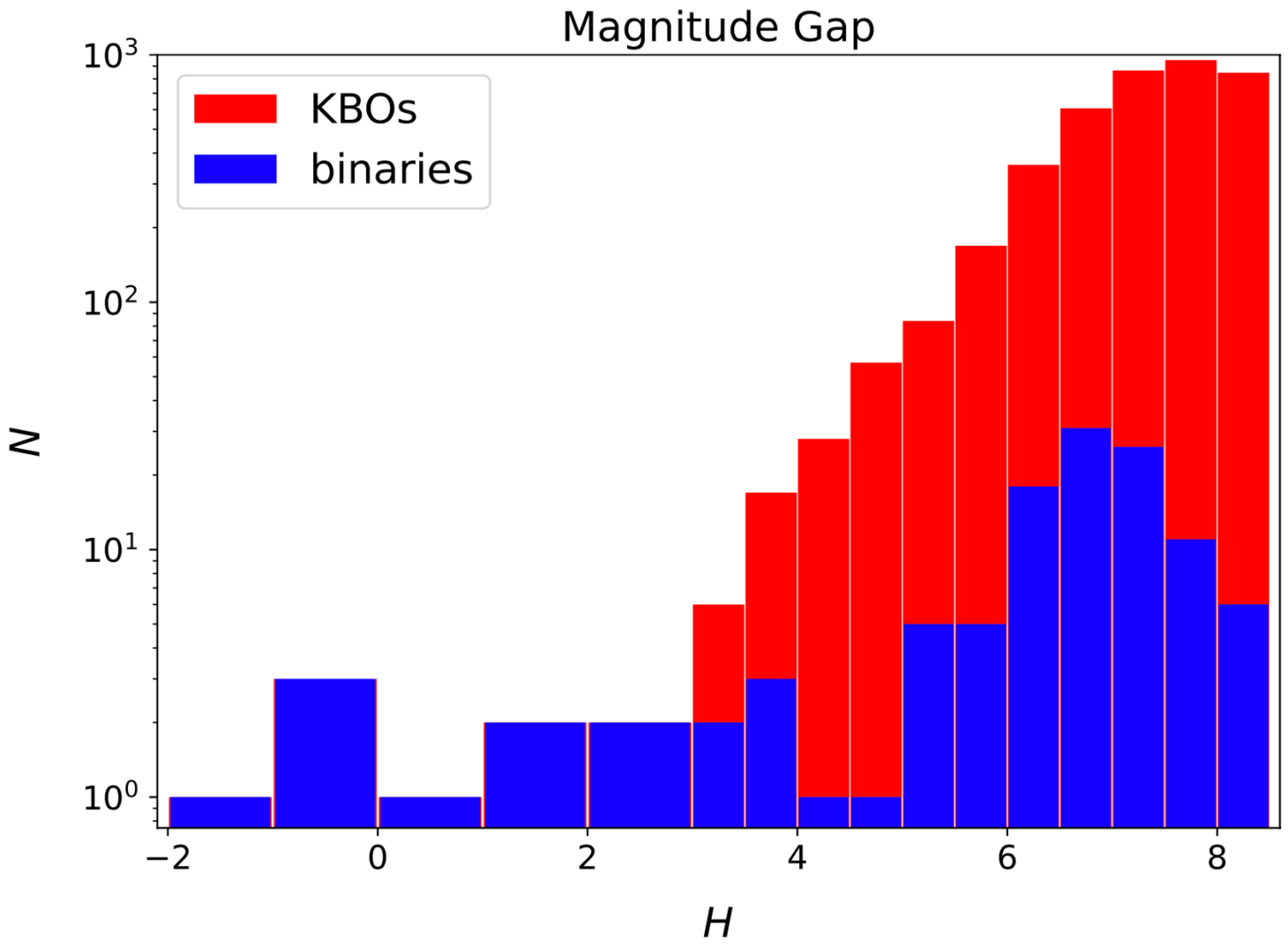

Lyra (2025)

Non-Keplerian orbits

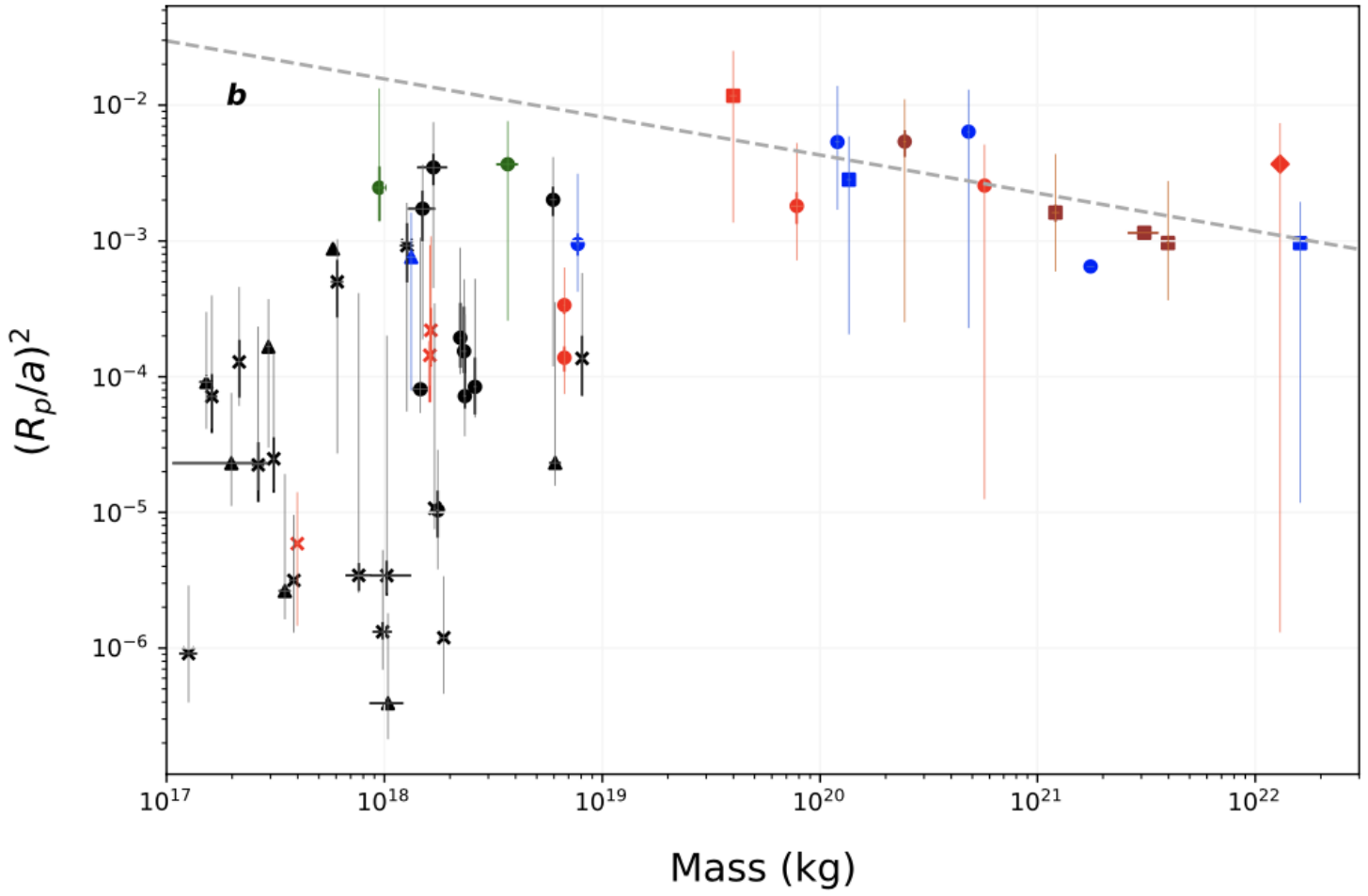

Lyra (2025)

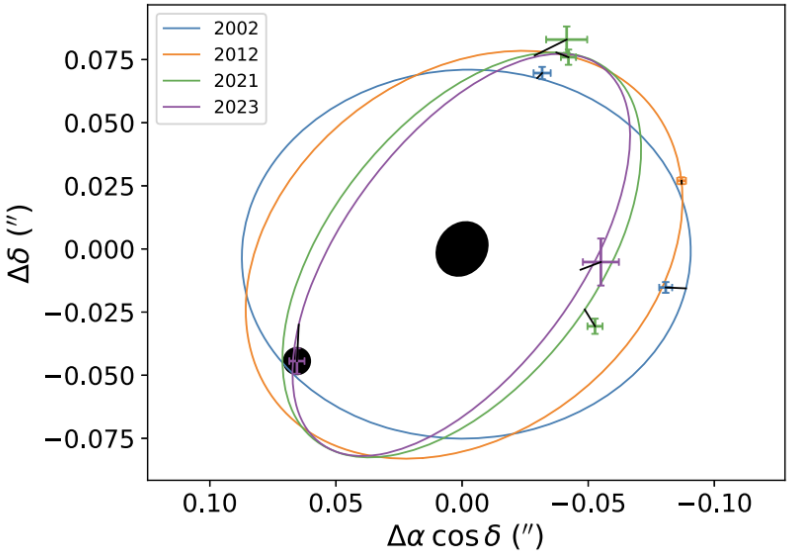

Rommel et al. (2025)

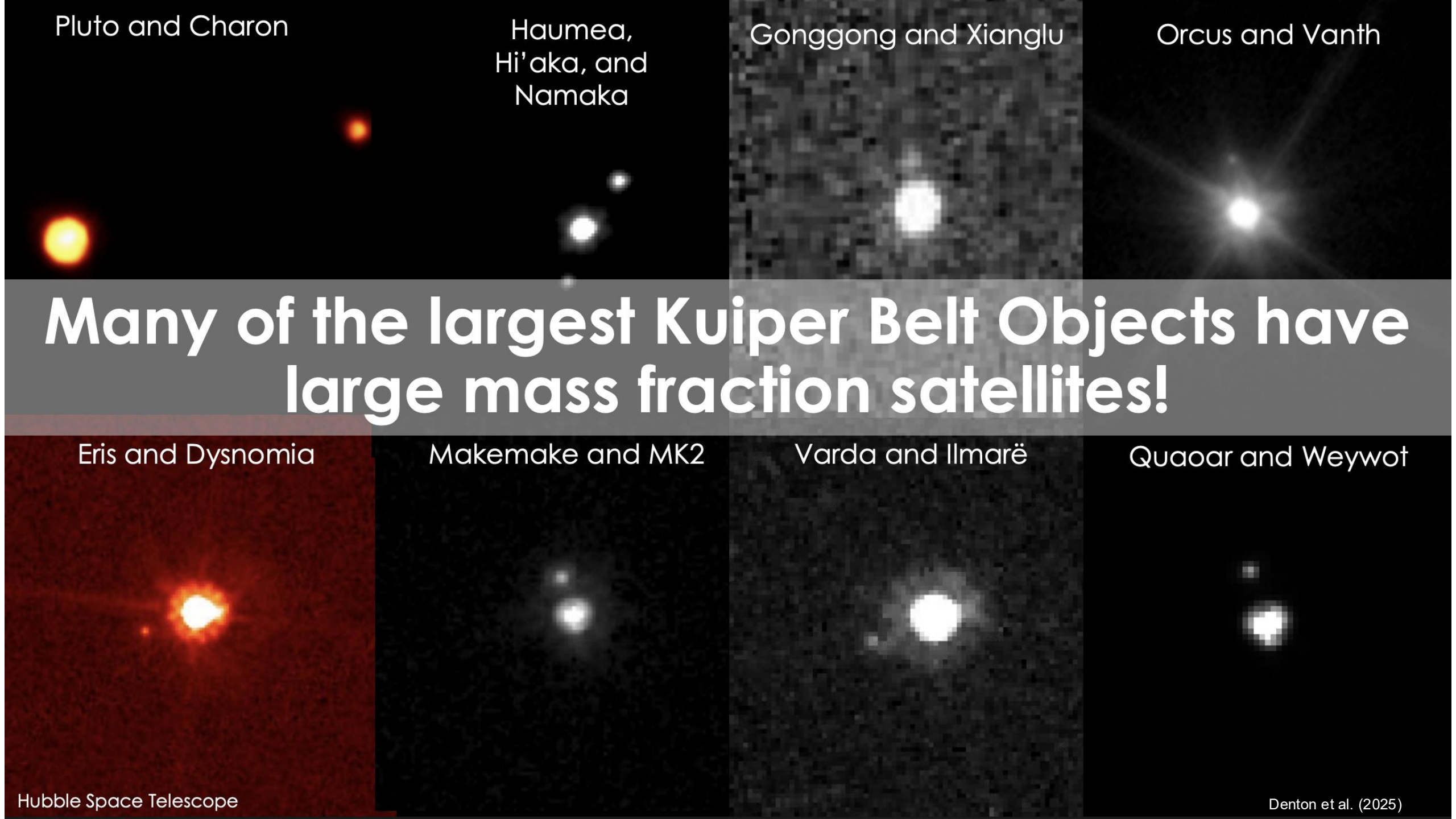
Pluto and Charon
Haumea, Hi'aka, and Namaka
Gonggong and Xianglu
Orcus and Vanth
Many of the largest Kuiper Belt Objects have large mass fraction satellites!
Eris and Dysnomia
Makemake and MK2
Varda and Ilmarë
Quaoar and Weywot
Hubble Space Telescope
Denton et al. (2025)

Different system architecture

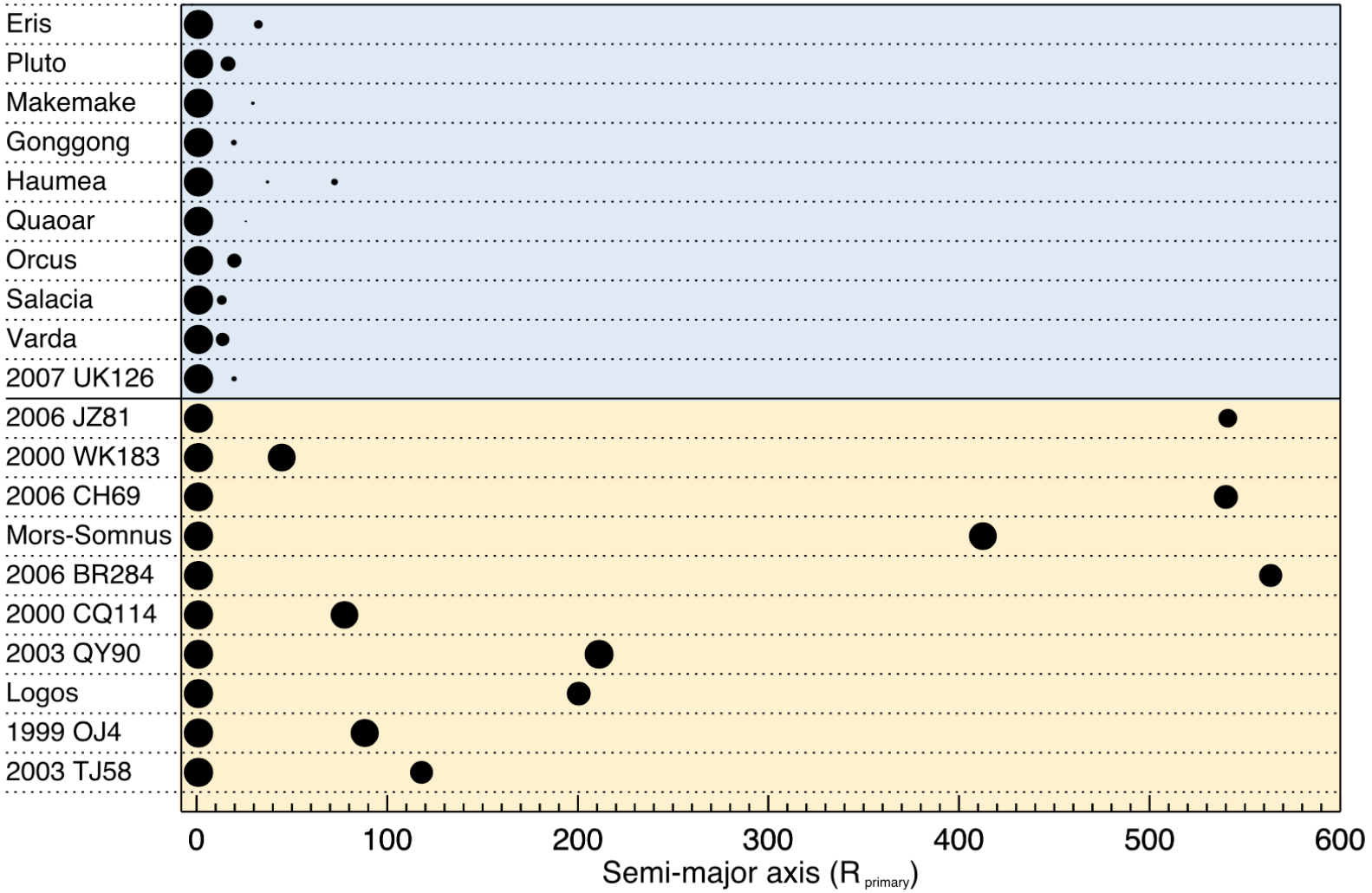

Bernstein et al (2023)

Did the high-mass objects lose their primordial satellites?

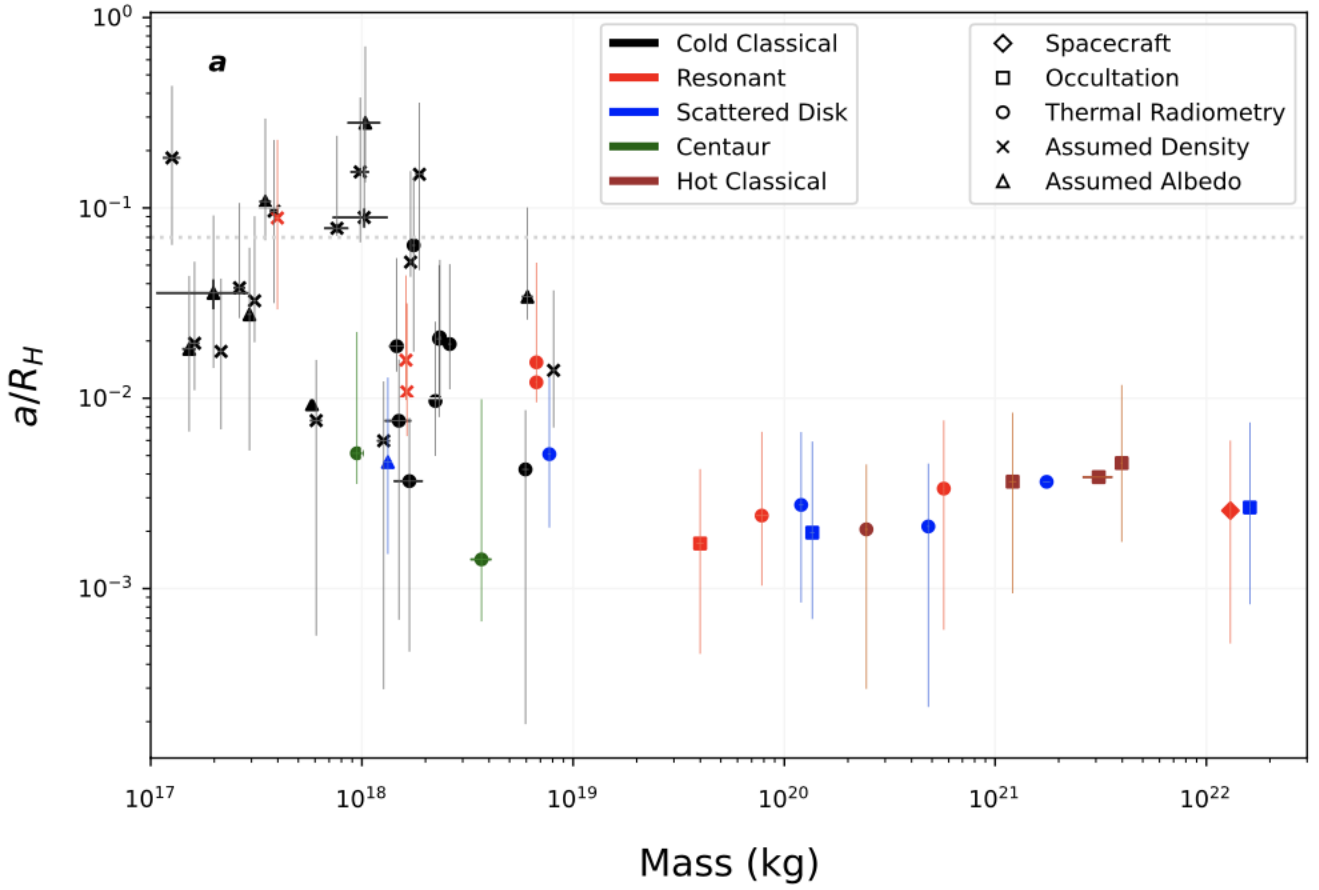

UWBs

Lyra (2025)

Satellites

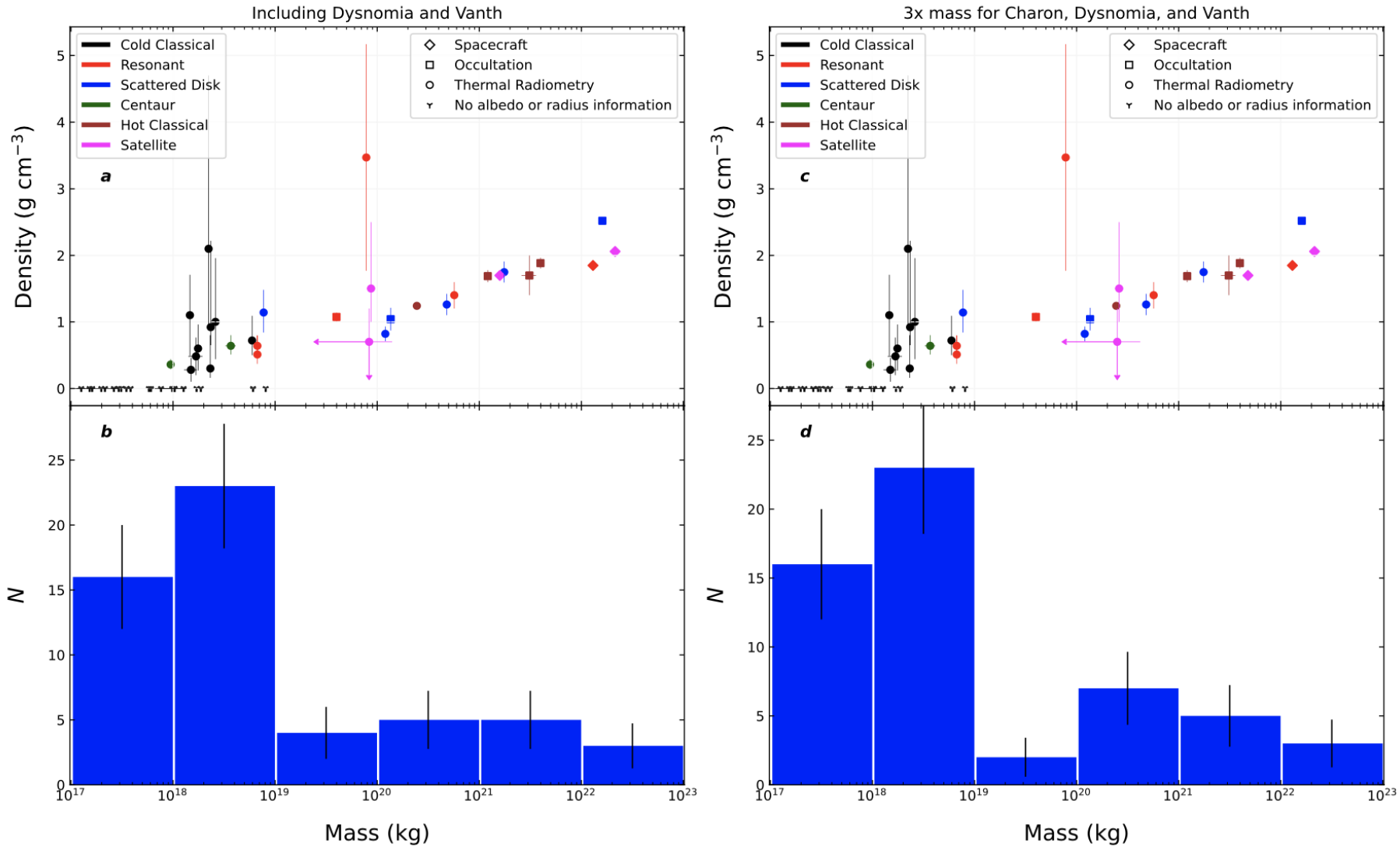

Lyra (2025, but see Denton et al. 2025 for lower mass ratios)

Pluto-Charon without strength high loss of mass scenario

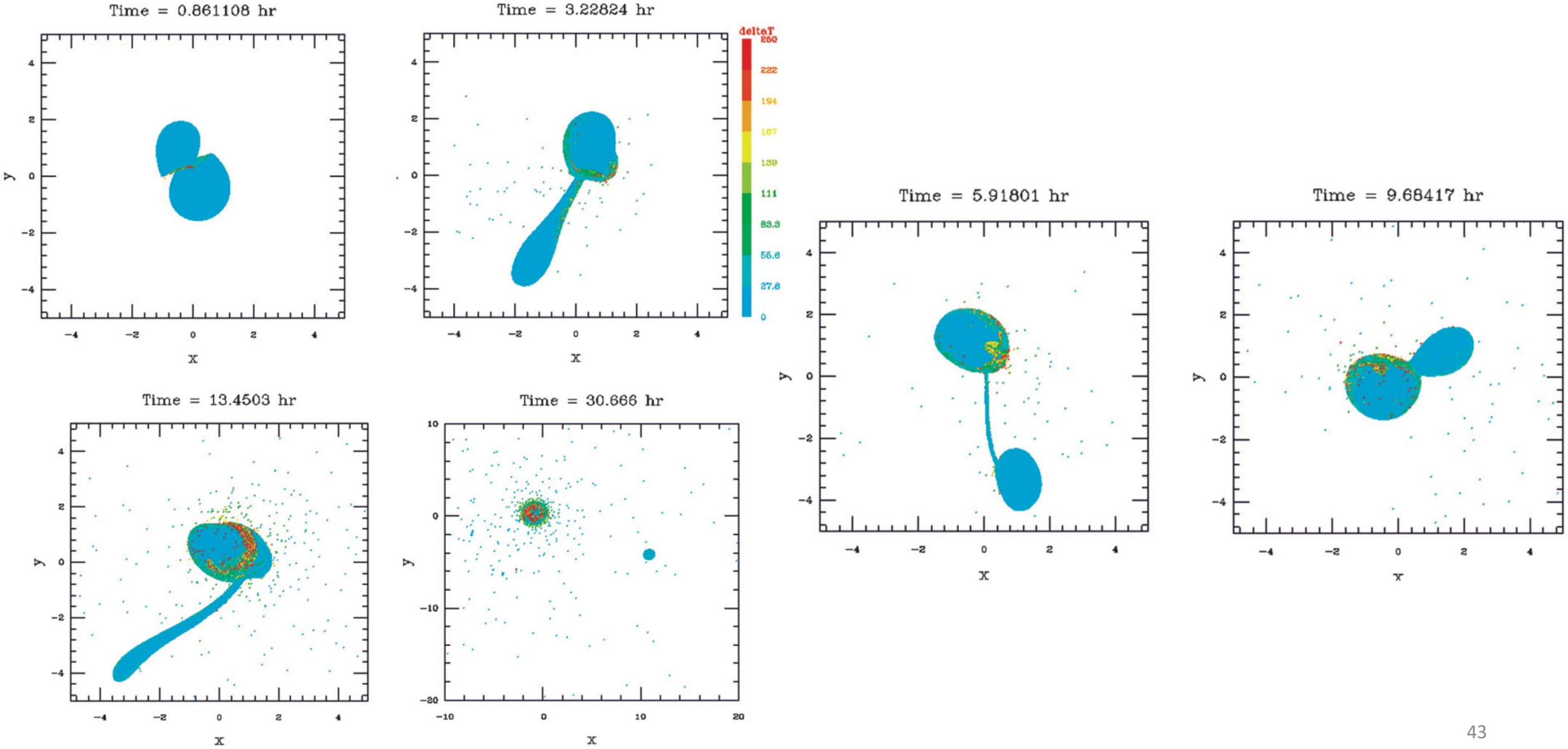

Canup (2011)

Pluto-Charon with strength “kiss and capture” low loss of mass scenario

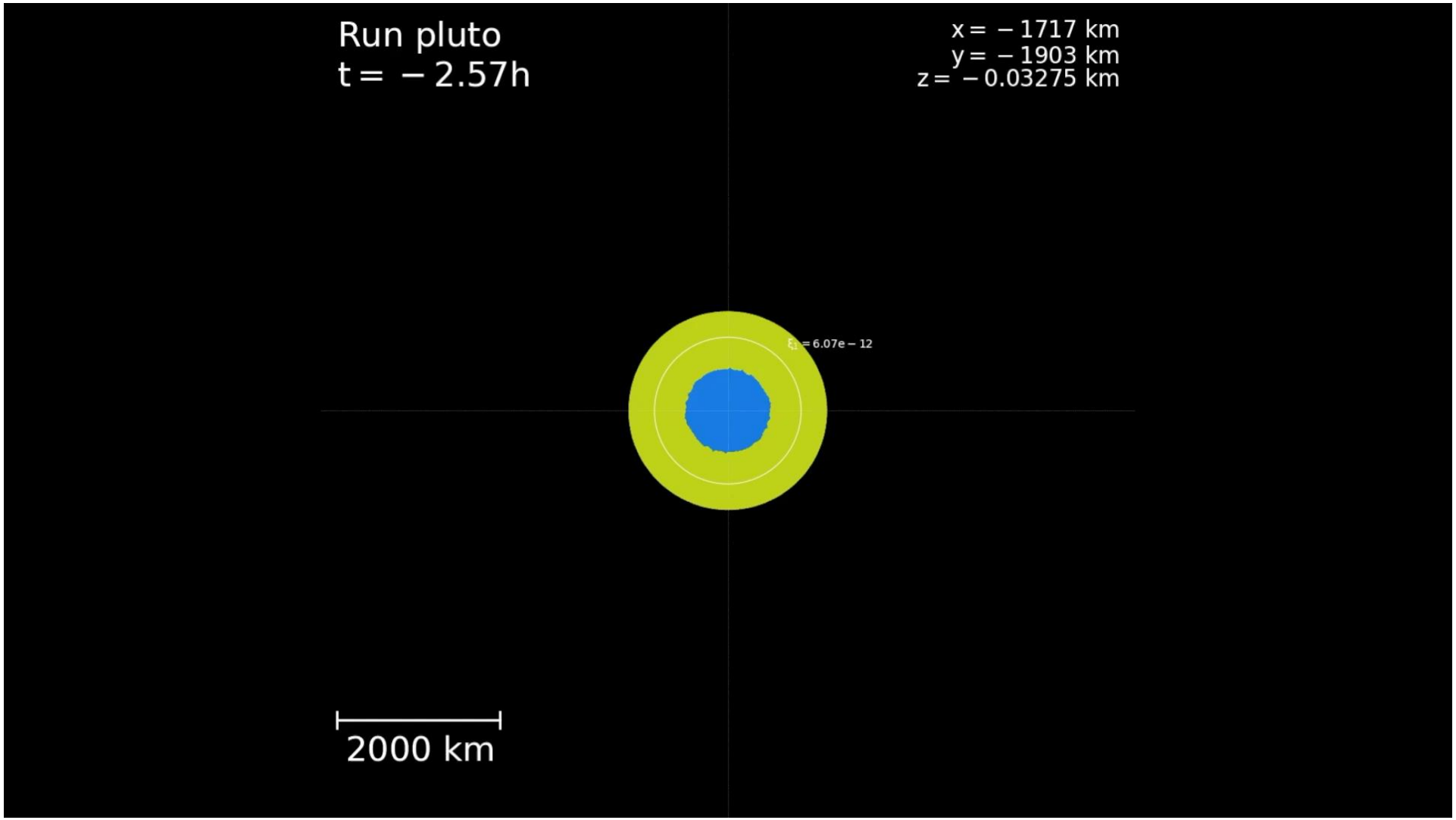

Denton et al. (2025)

Conclusions

- KBO density problem:
  - Two different pebble populations, maintained by ice desorption off small grains
  - Streaming instability: icy-rich small objects; nearly uniform composition
  - Pebble accretion: silicate-rich larger objects; varied composition
  - Melting avoided by
    - ice-rich formation
    - ^{26}Al incorporated mostly in long (>Myr) phase of silicate accretion
  - KBOs best reproduced between 15-25 AU
- Missing Binaries
  - Cold classicals capped at 10^{-3} Pluto masses
  - Gap between 10^{-3} and 10^{-2} Pluto masses for non-cold classicals
    - Formation imprint?
    - Dynamical loss?
    - Observation bias?